

FC  
USGS  
OFR  
80-1060

UNITED STATES  
DEPARTMENT OF THE INTERIOR  
GEOLOGICAL SURVEY

CONTINUED SEISMIC MONITORING OF THE GEYSERS, CALIFORNIA  
GEOTHERMAL AREA

UNIVERSITY OF UTAH  
RESEARCH INSTITUTE  
EARTH SCIENCE LAB.

authors:

R. S. Ludwin and C.G. Bufe

principal contributors:

V. Cagnetti

M. Stickney

C. Scofield

R. Robson

Open-File Report No. 80-1060

This report is preliminary and has not been edited or reviewed for conformity with Geological Survey standards and nomenclature.

## Table Of Contents

Abstract	1
Introduction.....	1
Objectives.....	4
Geothermal Development.....	5
Variation in Hypocenters with Time.....	8
Fault Plane Solutions.....	27
Stress Drops.....	30
Moments.....	31
Seismic Deformation.....	35
Geodetic, Gravity, and Reservoir Pressure Changes and Seismic Moment..	36
Temporal Variations in Seismicity.....	39
Conclusions.....	44
References.....	46
Acknowledgements.....	50

## Figures

1. Regional seismicity map.....	3
2. Map of the steam field.....	6
3. Plots showing detailed seismic activity as a function of time.....	10
3A. 1972-5/75 seismicity at The Geysers, map view and X-section.....	11
3. 5/75-10/75 seismicity at The Geysers....."	12
3C. 11/75-4/76 seismicity at The Geysers....."	13
3D. 5/76-10/76 seismicity at The Geysers....."	14
3E. 11/76-4/77 seismicity at The Geysers....."	15

3F.	5/77-10/77 seismicity at The Geysers....."	16
3G.	11/77-4/78 seismicity at The Geysers....."	17
3H.	5/78-10/78 seismicity at The Geysers....."	18
3I.	11/78-4/79 seismicity at The Geysers....."	19
3J.	5/79-10/79 seismicity at The Geysers....."	20
3K.	11/79-4/80 seismicity at The Geysers....."	21
4.	Map of The Geysers events located by Majer and McEvilly (1979)...	24
5.	Numbers, b-values and moment sums versus depth.....	25
6.	Map view of fault plane solutions for events of $M_c \geq 2.5$ .....	28
7.	P and S wave moment-magnitude relations.....	32
8.	Gravity, geodetic and pressure changes, shown with moment sum along A-A' (figure 2).....	38
9.	Statistical analysis of The Geysers and the region surrounding it, steam production.....	41
10.	Maximum annual event and steam production.....	43

Tables

table 1.	.....	7
	Events/year per $\text{km}^2$ , b-values, moment rate per $\text{km}^2$ , and beginning dates for power producing zones and injection wells shown in figure 2. Megawatts are given for power plants, and depths for injection wells.	
table 2.	.....	29
	Times, locations, depths, magnitudes, and RMS p-wave travel-time residuals for events of $M_c \geq 2.5$	

## Abstract

Probable effects of geothermal development on seismicity at The Geysers are shown by the spatial coherence of decreases in gravity and pressure with maximum geodetic deformation and seismic moment sum along a line through the most developed area of the geothermal field. Increases in the mean number of events per day and in the magnitude of largest annual event correlate with increases in steam production. The two largest earthquakes in the steam field occurred near the two injection wells most distant from production wells, and large events ( $M_o \geq 2.5$ ) occurred most frequently during months of peak injection. Spatial seismic clusters in proximity to injection wells have occurred soon after injection began. Preliminary data also indicate an increase in seismicity in a previously aseismic area near plant 15 following the beginning of power production at that plant in 1979.

## Introduction

The Geysers is currently the site of the largest geothermal power development in the world (more than 800 megawatts) and the only one in the United States. Located in California 130 km north of San Francisco in Lake and Sonoma Counties, the steam reservoir consists of a massive fractured graywacke. The graywacke, part of the Franciscan assemblage, is capped by impermeable ultramafic and metamorphic rocks also of the Franciscan. Structurally, the presently producing steam field lies on the north-east limb of a south-east plunging antiform (McLaughlin, 1977). Immediately to the north of The Geysers

are the Clear Lake Volcanics, the most recent of the Coast Range Volcanics, with eruptions dating from less than 2.05 million years to less than .03 million years (Hearn, Donnelly and Goff, 1976).

The period of volcanic activity at The Geysers is briefest in duration as well as youngest of the Coast Range Volcanics. This brevity, a lack of extensive ash flows, and an absence of collapse calderas may indicate that the present volcanic quiescence is only a hiatus (Hearn, Donnelly and Goff, 1976).

The heat source for The Geysers is believed to be a magma body at a depth of about 6-30 km. This hypothesis is supported by several lines of geophysical evidence. About 15 km northeast of the producing steam field a residual gravity low of approximately 30 mgal with a diameter of about 20 km is centered over Mount Hannah. A second smaller, gravity low of -20 mgal lies over the steam production field (Isherwood, 1976). These gravity lows (figure 1) are unassociated with long wavelength magnetic anomalies from deep sources, and have been modeled as a shallow magma body with temperature above the Curie point and density lower than the surrounding rock (Isherwood, 1976) which may extend beneath the steam production field at The Geysers (Iyer, Oppenheimer, and Hitchcock, 1979). Teleseismic P-waves recorded at stations in the Clear Lake volcanic field show delays of up to 1.5 sec. which cannot be accounted for by velocity anomalies shallower than 3 km and suggest extreme variation in properties of underlying materials (Iyer, Oppenheimer and Hitchcock, 1979). These teleseismic delays are consistent with a partially molten, low-velocity body of size and depth comparable to that suggested by gravity data (figure 1). Additionally, all seismic events at The Geysers with

# GEYSERS-CLEAR LAKE REGION

5/75-5/79

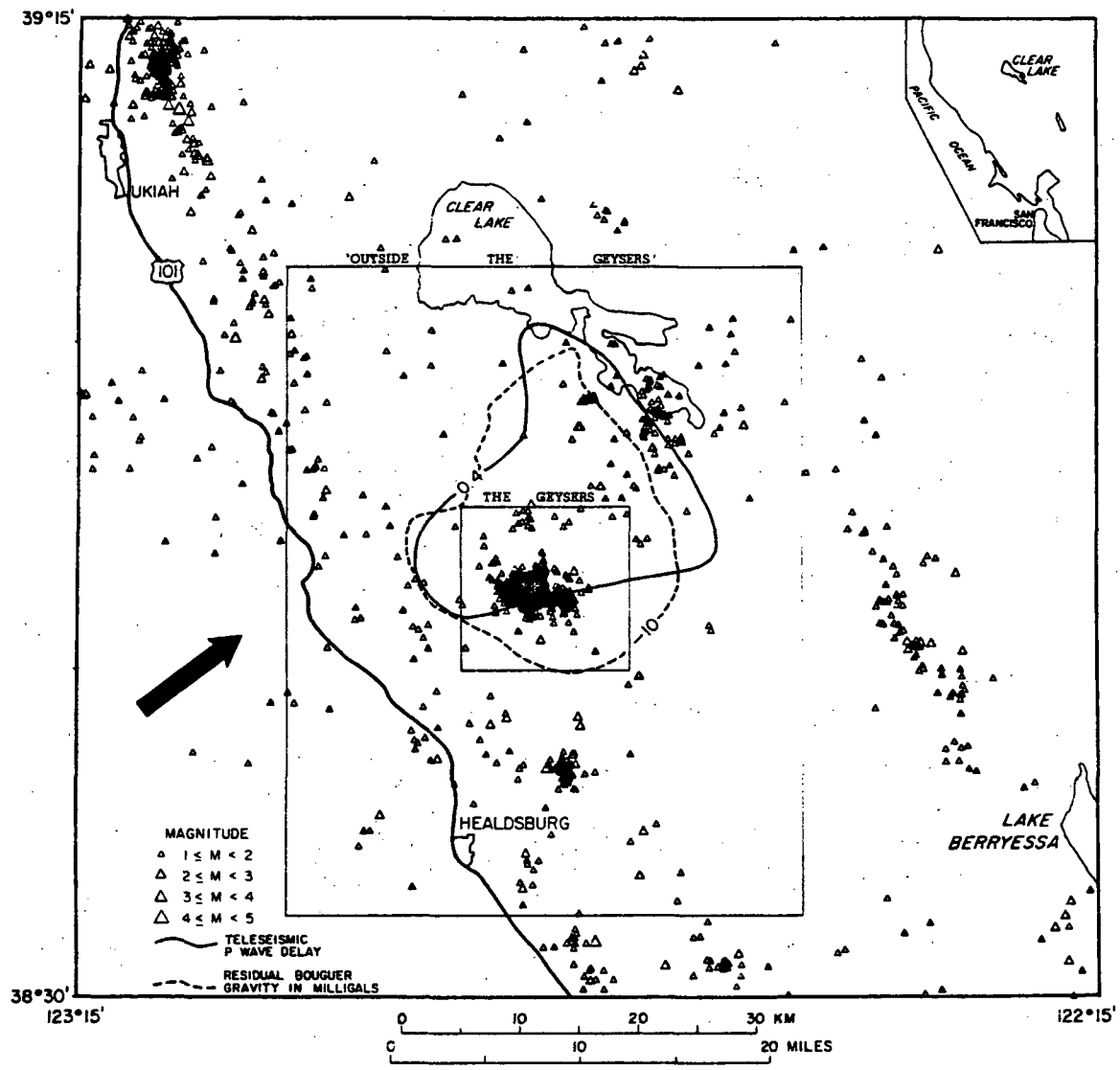


Figure 1. Seismicity at The Geysers and in the surrounding region 5/75 - 5/79. Seismic activity in boxed areas 'Outside The Geysers' and The Geysers was analyzed statistically. Bouguer residual gravity anomaly is shown as a dotted line, the -10 mgal contour shown surrounds both the -30 mgal anomaly centered on Mt. Hannah (north of The Geysers) and the smaller gravity low over the steam production field. Teleseismic P-wave delays are represented by the 0.4 second contour for a teleseism arriving from the southwest, shown as a solid line.

well-constrained depths are shallower than 5 km (Marks et al., 1977). This suggests that below 5 km the rock may respond to strain in a plastic manner, again consistent with a molten or partially molten body at depth.

Earthquake epicenters north of San Francisco in a zone showing The Geysers, Clear Lake, and Lake Berryessa are shown in figure 1. The seismic activity is comprised of the cluster of events at The Geysers, a small cluster at the southeast end of Clear Lake, and alignments of hypocenters along the Maacama fault to the west and an unnamed fault (intermediate between the Green Valley and Collayomi faults) to the east, both trending northeast to southwest. Ten km south of The Geysers a swarm of events occurred in September 1977 at Alexander Valley. Ukiah, northeast of The Geysers, was the scene of a mainshock-aftershock sequence (largest event  $M_c = 4.4$ ) in March 1978.

### Objectives

The objectives of our study of The Geysers are:

1. Presentation of hypocentral maps and cross-sections showing the spatial relation of earthquake activity to production and injection wells.
2. Detailed monitoring of present level of microearthquake activity in the vicinity of power plants 12, 13, 14, and 15.
3. Statistical examination of seismicity fluctuations at The Geysers and comparison with rates of steam withdrawal.
4. Estimation of spatial and temporal variation in principal stress orientation from fault plane solutions for selected events in The Geysers-Clear Lake region.

5. Updated estimates of rate of local deformation from cumulative seismic moment to determine whether integrated effects of continued seismicity pose a long-term threat to installations at The Geysers.
6. Comparative spectral studies to determine whether source dimension, moment, and stress drop of earthquakes in the production area are outside the range of those for "natural" earthquakes of equivalent magnitude in the surrounding region.

### Geothermal Development

Geothermal development at The Geysers consists of turbines turned by steam pressure. Steam is provided by wells ranging in depth from 0.16 to 2.90 km. Each turbine is referred to by number, and two turbines may be located in the same building. Allusions to "power plant 1 & 2," etc., mean that turbines 1 and 2 share a building. Power plant locations and corresponding zones from which steam is produced are shown in figure 2. Zones serving units 1-12 and 14 are based on information from Union Oil Company, while zones near plants 13 and 15 are based on production well positions.

Power plant shutdowns are generally due to either scheduled maintenance or operating difficulties. Because of the lower operating costs relative to fossil fuel plants, power production cutbacks are minimized unless an unusually abundant source of hydroelectric power is available, as in the spring of 1978. Attempts to correlate power plant shutdowns and seismic activity have yielded inconclusive results. When a power plant is down, steam can be rerouted to other plants, so that a plant shutdown and steam production



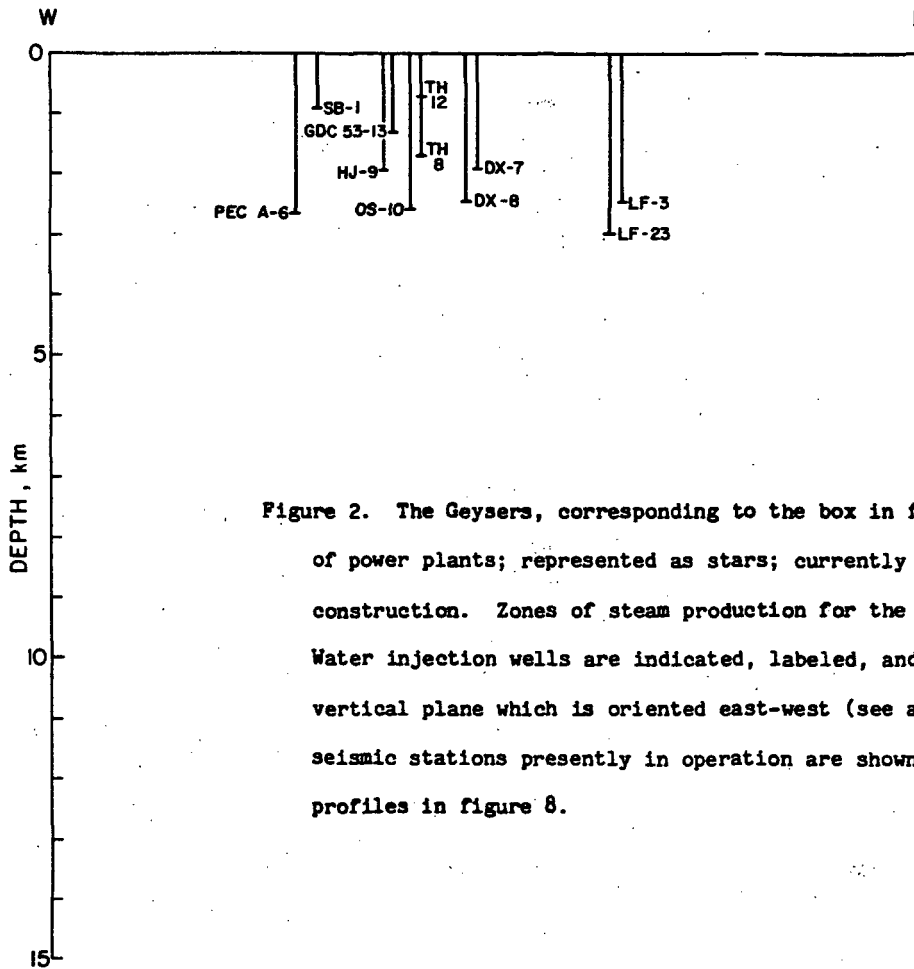
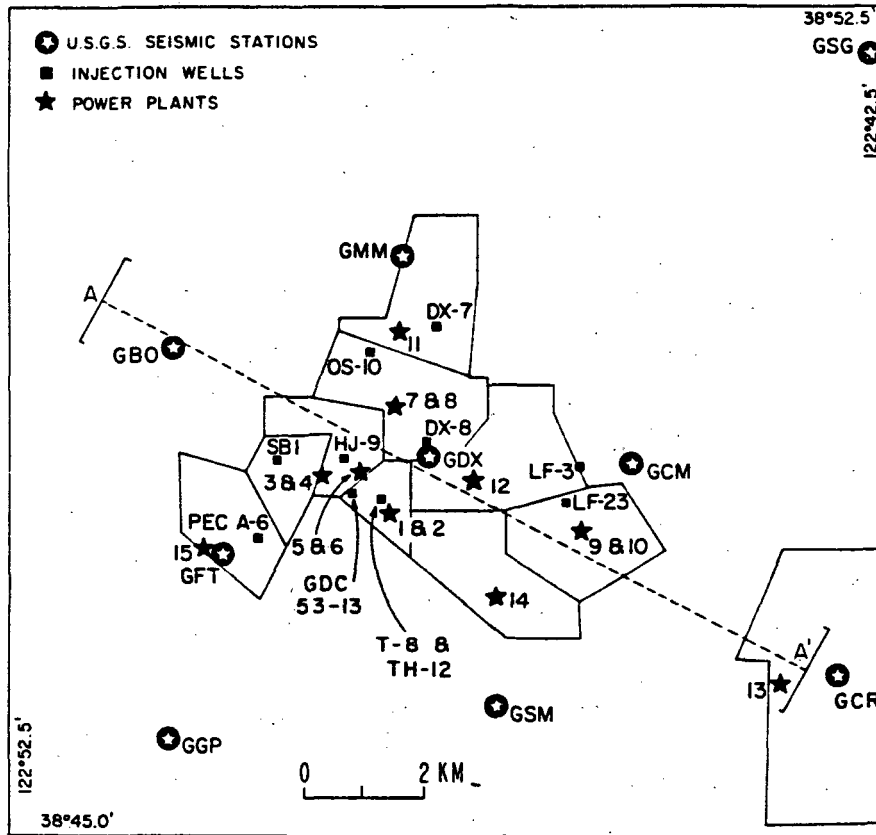


Figure 2. The Geysers, corresponding to the box in figure 1. Locations of power plants; represented as stars; currently producing or under construction. Zones of steam production for the plants are outlined. Water injection wells are indicated, labeled, and shown projected onto a vertical plane which is oriented east-west (see also table 1). U.S.G.S. seismic stations presently in operation are shown. Line A-A' refers to profiles in figure 8.

Table 1

Events of  $M_c \geq 1.1$  5/75-11/78  
 $\text{Log } M_0 = 16.7 + 1.3 M_c$

A. POWER PLANTS

<u>Number</u>	<u>Date of commercial operation</u>	<u>Megawatts</u>	<u>Events/Year per km<sup>2</sup></u>		<u>Moment sum/Year per km<sup>2</sup></u> <u>X 10<sup>19</sup> dyne-cm</u>
			<u><math>M_c \geq 1.1</math></u>	<u>b-value</u>	
1	09/25/60	12.5	36	1.22	40.00
2	03/19/63	13.8			
3	04/28/67	27.5	15	1.26	11.39
4	03/02/68	27.5			
5	12/15/71	55	25	1.39	16.10
6	12/15/71	55	55		
7	08/18/72	55	25	1.05	24.72
8	11/23/72	55			
9	10/25/73	55	4	1.24	2.73
10	11/30/73	55			
11	11/20/75	110	1	1.04	4.28
12	03/01/79	110	12	1.33	9.96
13	05/15/80	140	0	-	-
14	08/--/80*	110	1	1.14	.71
15	06/17/79	55	0	-	-

\*planned

B. INJECTION WELLS

<u>Name</u>	<u>Begin date</u>	<u>End date</u>	<u>depth km</u>	<u>Events/Year per km<sup>2</sup></u>	<u>b-value</u>	<u>Moment sum/Year per km<sup>2</sup></u> <u>X 10<sup>19</sup> dyne-cm</u>
SB1	04/10/69		.90	12	1.24	6.15
TH12	08/23/70	intermittant	.72	8	.96	11.28
TH8	05/03/71		1.70	35	1.08	56.38
LF3	09/11/73		2.44	5	.55	53.84
DX8	10/03/74		2.45	40	1.12	44.34
OS10	12/03/74		2.59	7	1.32	2.89
DX7	12/22/75		1.89	3	.62	25.95
HJ9	11/11/78		1.86			
GDC-53-13	03/30/79		1.30			
LF23	04/08/79		3.02			
PEC A-6	06/01/79		2.66			

in that part of the field are not necessarily related.

Geothermal activity at The Geysers consists of steam fumaroles rather than true geysers. The existence of steam suggests that water inflow is restricted. Annual fluid recharge of the reservoir has been estimated at close to zero (Nur et al., 1978). In an attempt to slow depletion of the reservoir, cooling towers condense as much steam as possible, and condensate is introduced into the steam producing formation by injection wells.

Development currently entails removal of more than  $6.5 \times 10^6$  kg of mass per hour (Reed, 1976), and approximately 1/3 of this mass is condensed and reinjected at a few wells. Injection wells range in depth from 0.90 to 3.02 km and are shown in map view and cross section in figure 2. Table 1 gives the years injection began, numbers of events per square km per year, b values, and seismic moment sum per square km per year for square areas (.75 km x .75 km) around injection wells. Since most of the injection wells are surrounded by older production wells, separation of effects due to steam withdrawal and condensate injection is difficult. Two injection wells, DX-7 and LF-3, lie outside steam production zones, providing an opportunity to isolate seismicity associated with fluid injection. The two largest earthquakes at The Geysers, Richter magnitudes 3.8 (Dec. 22, 1976) and 3.5 (Sept. 22, 1977), occurred in proximity to wells LF-3 and DX-7 respectively. Few smaller events occurred near these injection wells.

#### Variation in Hypocenters with Time

The most striking feature of seismic activity at The Geysers is the spatial

consistency of the seismic cluster through time, as seen in figure 3. Figure 2 has been reproduced on a transparency (in pocket of back cover) so that it may be overlaid on figures 3 and 6. Prior to May of 1975, hypo-central locations were poorly constrained (figure 3A) owing to the lack of local stations. In May of 1975, stations GBO, GCM, GGP, and GSM were added to the USGS Central California Seismographic Network (see figure 2), considerably improving location threshold and hypocenters. Station GDY, which lies in the approximate center of the western cluster (and the production area), was installed in November of 1977. Thus, the last five time periods (figures 3G-3K) have better depth control than the preceding five (figures 3B-3F). An additional station, GCR, was installed in May 1979 at Castle Rock Springs, to the east of the original steam production zone, near power plant 13.

Data represented in figures 3 since May 1975 are preliminary California Network hypocentral locations with P-wave RMS travel time residuals less than 0.30 sec and A and B quality solutions. Prior to 1975 all hypocentral locations are plotted. Magnitudes,  $M_c$ , computed by the USGS California Network are based on an empirical relation between coda length (signal duration) and Richter magnitude,  $M_L$ , for central California earthquakes (Lee et al., 1972). This relation appears to be applicable to earthquakes at The Geysers in the magnitude 1 to 3 range (Peppin and Bufe, 1980).

East-west cross sectional views of data from ten six-month time periods (figures 3B-3K) since May 1975 clearly show two separate clusters which roughly coincide with two independent regions of decreased steam pressure resulting from production (Lipman et al., 1978). The two clusters, and the gap which separates them, are visible in each of the time periods. The lack

Figure 3. Detailed seismic activity at The Geysers as a function of time.

Seismicity in each time period is shown in map view and projected onto a vertical, east-west striking plane. Also shown is the 500 psia isobar contour indicating the position of the pressure sink.

(A) January 1972 - April 1975

Data collected before installation of nearby stations.

Contours of the 500 psia isobar in 1972 and 1975 are shown.

(B - K) six month time periods; May 1975 - April 1979.

(B) May 1975 - Oct. 1975 showing 500 psia isobar contour from  
1975

(C) Nov. 1975 - April 1976 "

(D) May 1976 - Oct. 1976 "

(E) Nov. 1976 - April 1977 showing 500 psia isobar contour from  
1977

(F) May 1977 - Oct. 1977 "

(G) Nov. 1977 - April 1978 "

(H) May 1978 - Oct. 1978 "

(I) Nov. 1978 - April 1979 "

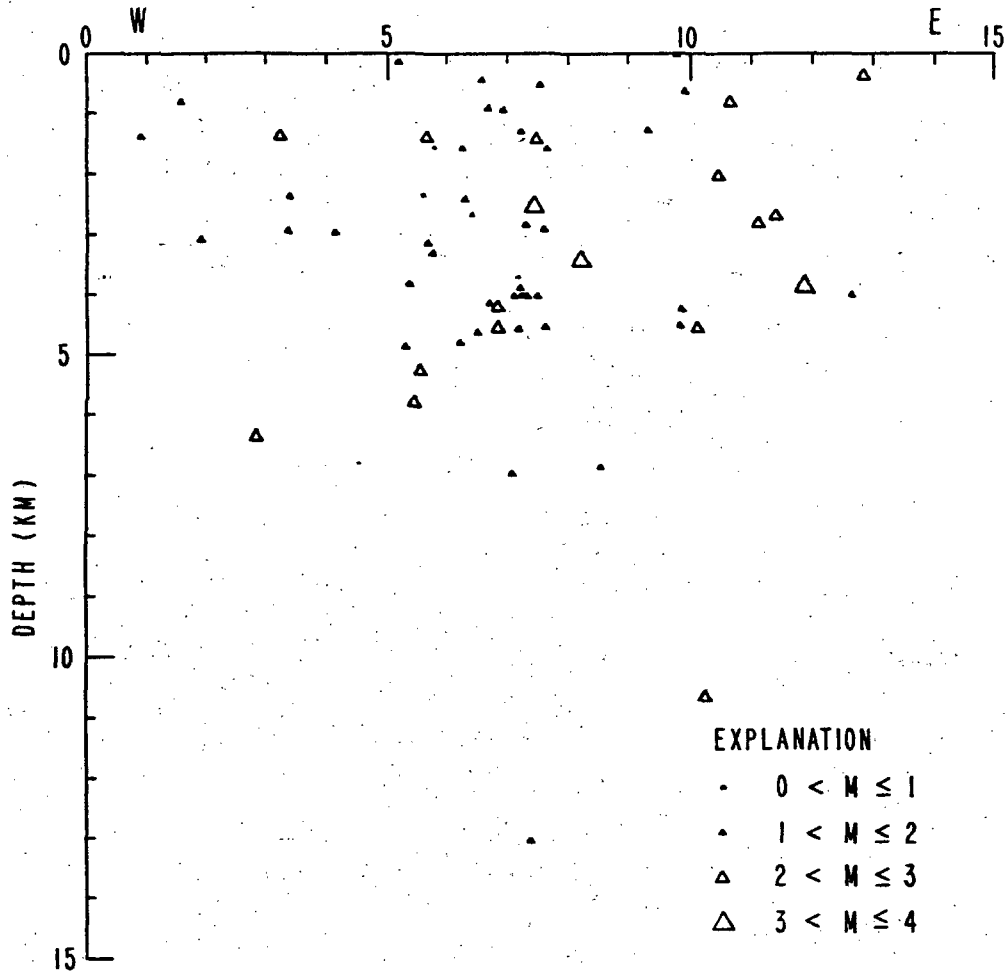
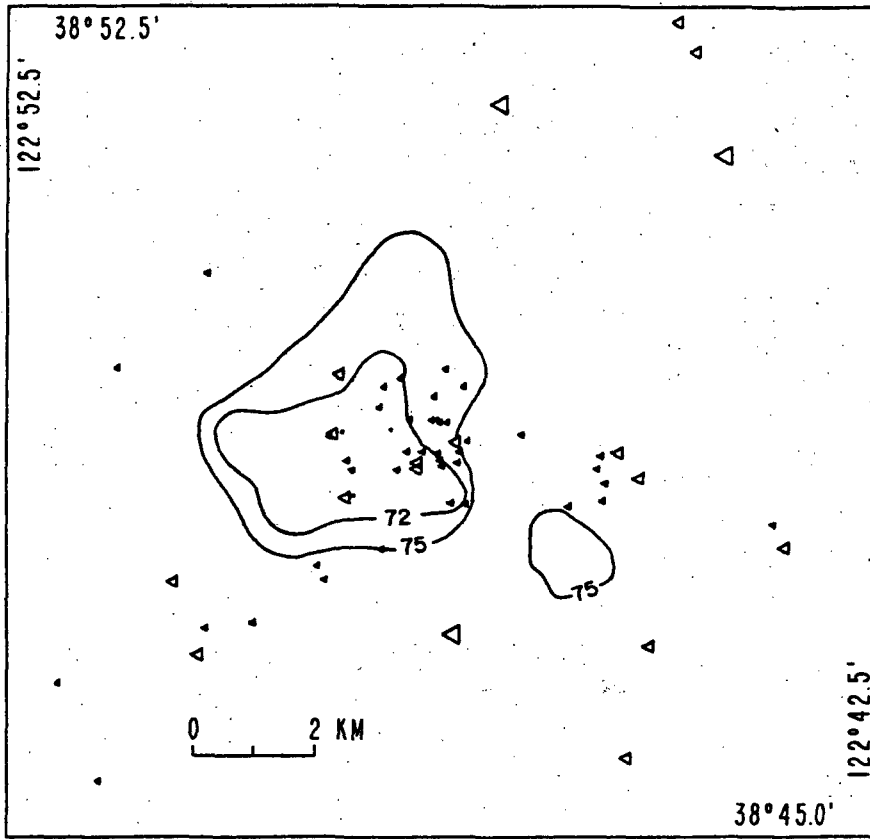
(J) May 1979 - Oct. 1979 "

(K) Nov. 1979 - April 1980 "

THE GEYSERS JANUARY 1972 — APRIL 1975

3-A.

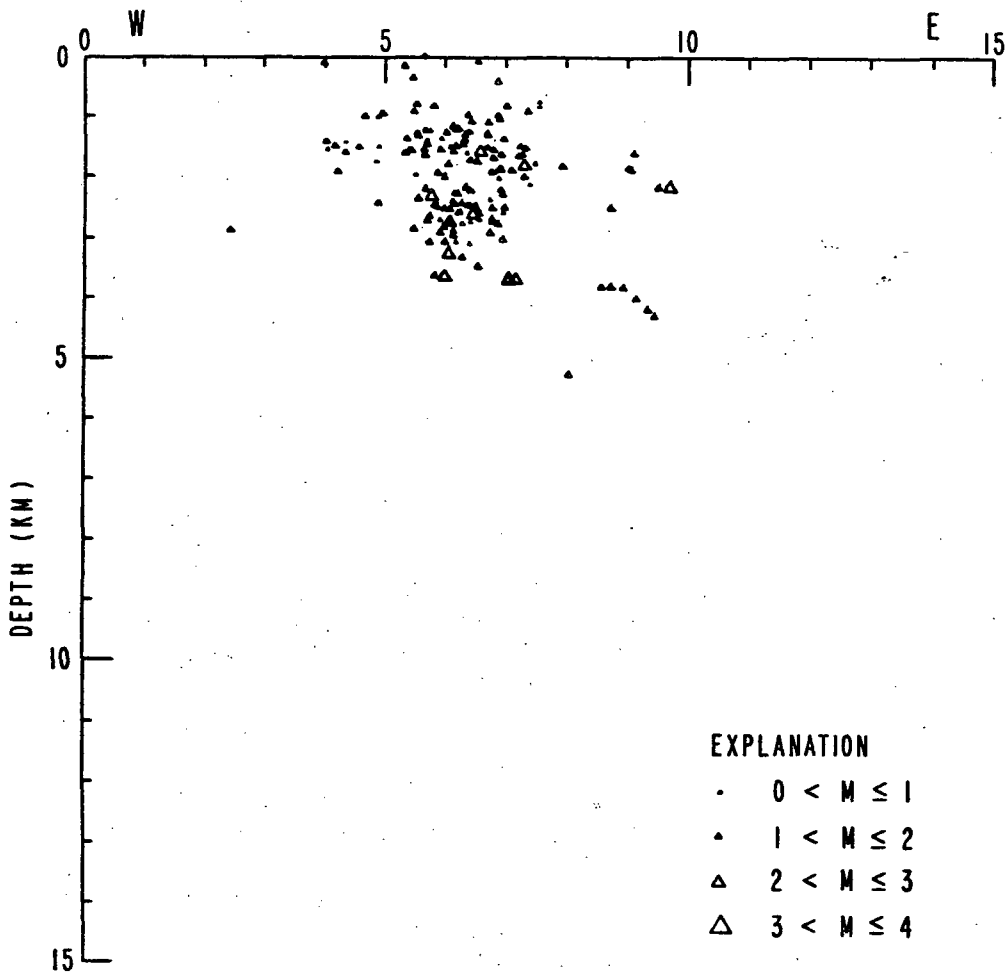
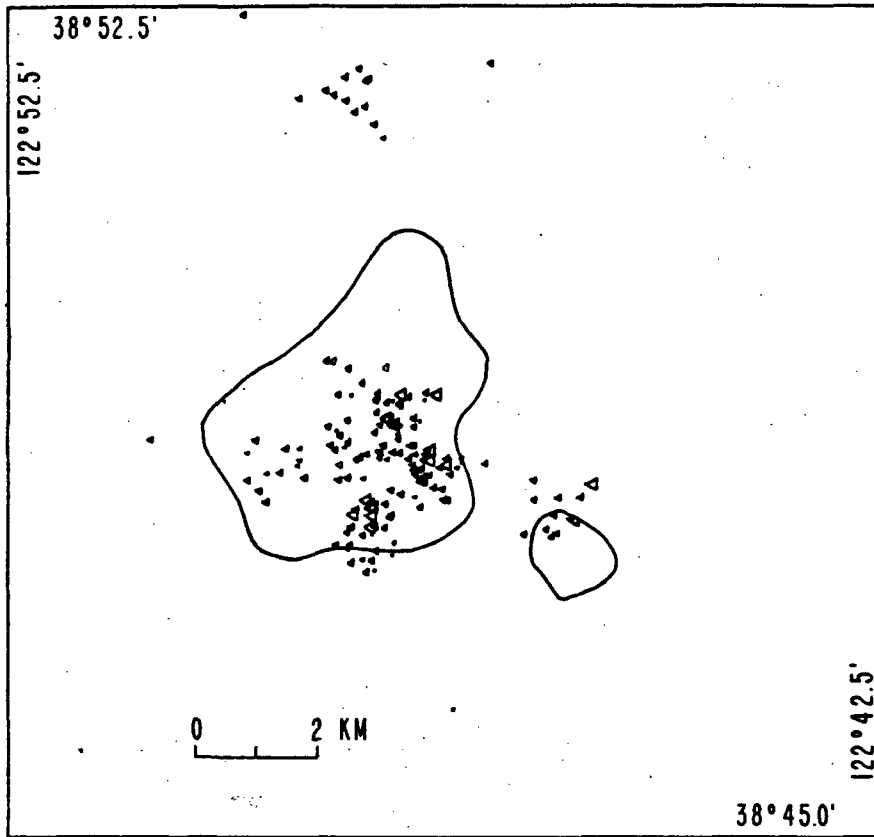
11



THE GEYSERS MAY 1975 - OCTOBER 1975

3-B.

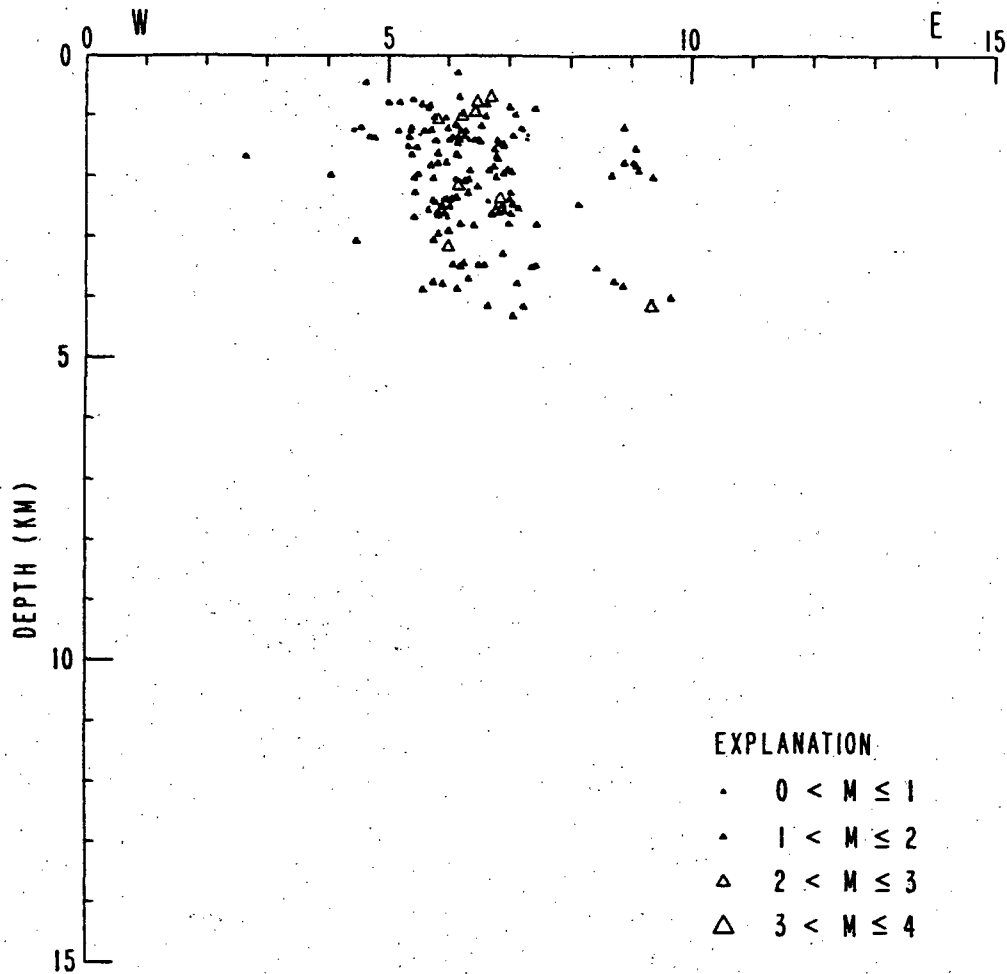
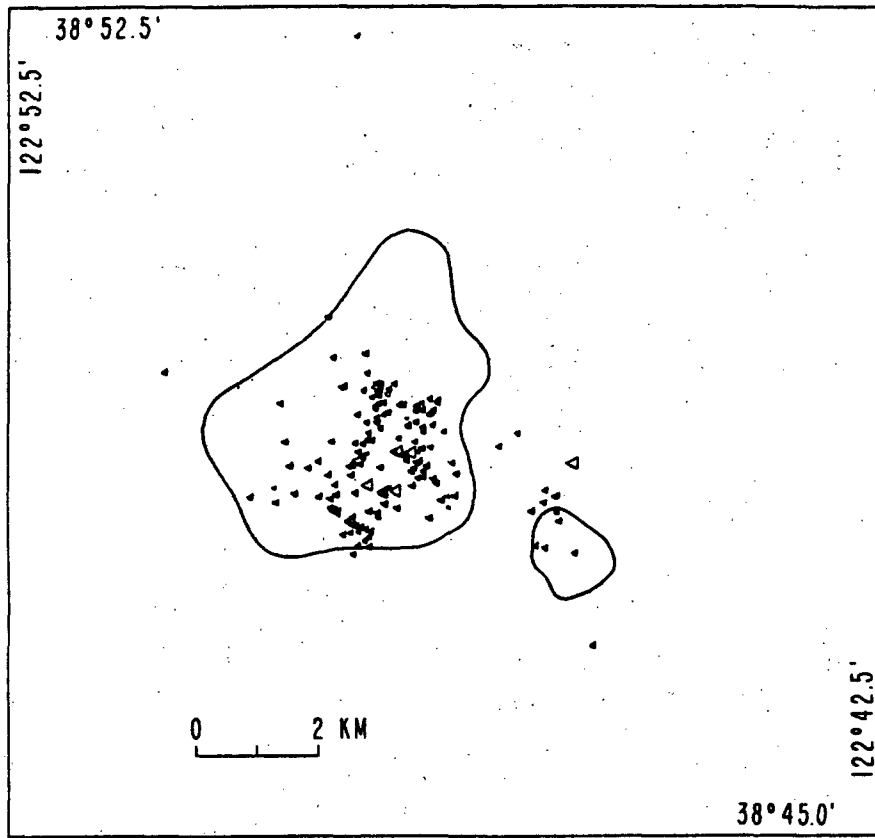
12.



THE GEYSERS NOVEMBER 1975 - APRIL 1976

13

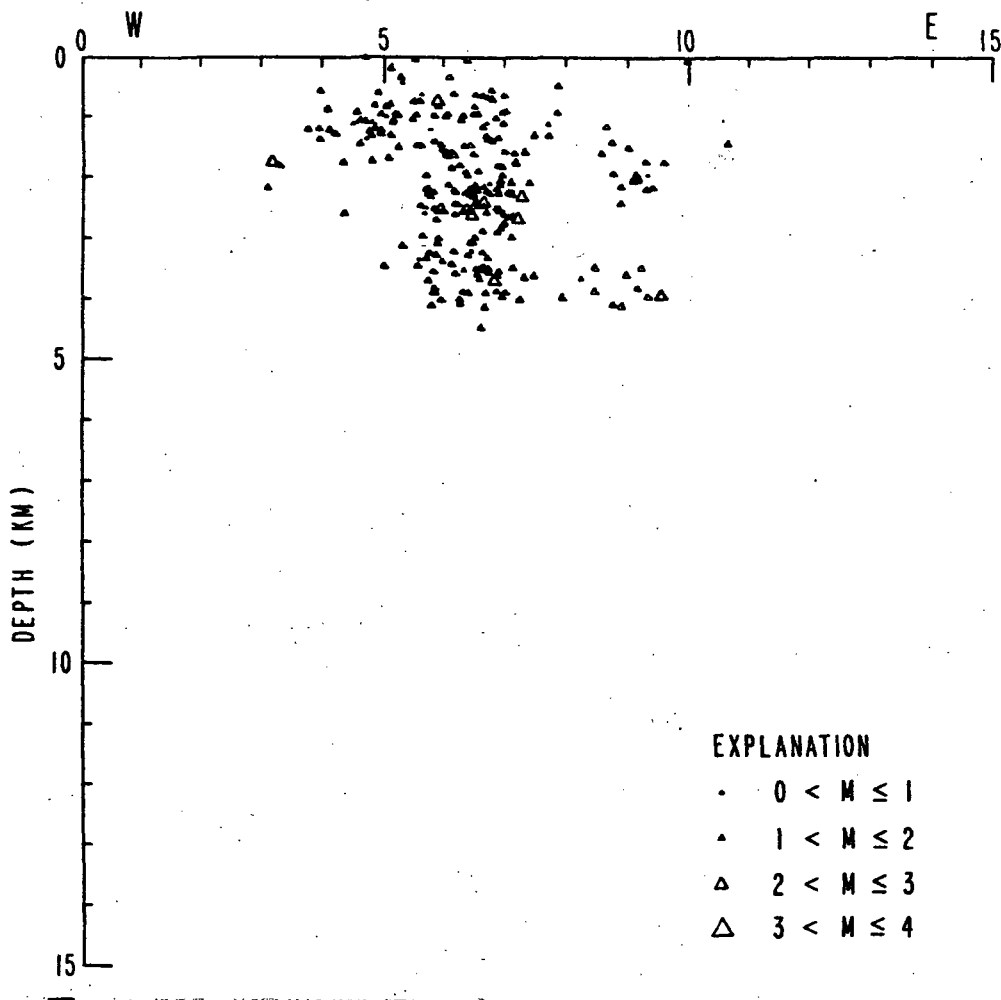
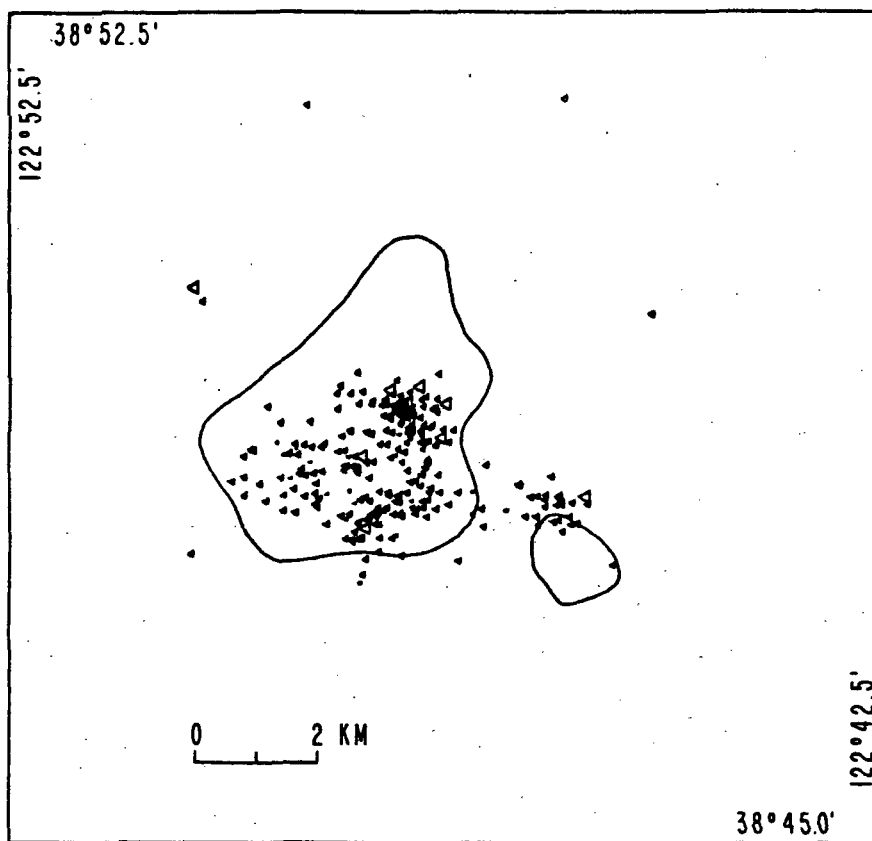
3-C.





THE GEYSERS MAY 1976 - OCTOBER 1976

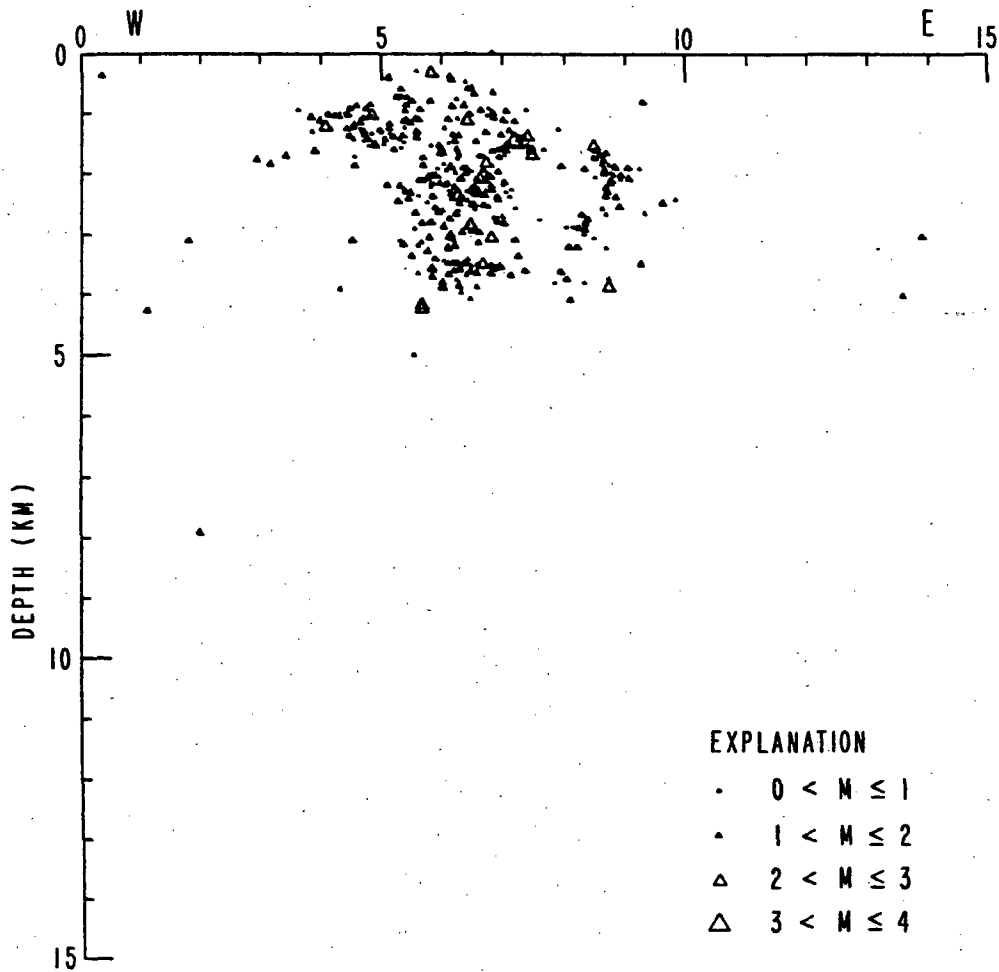
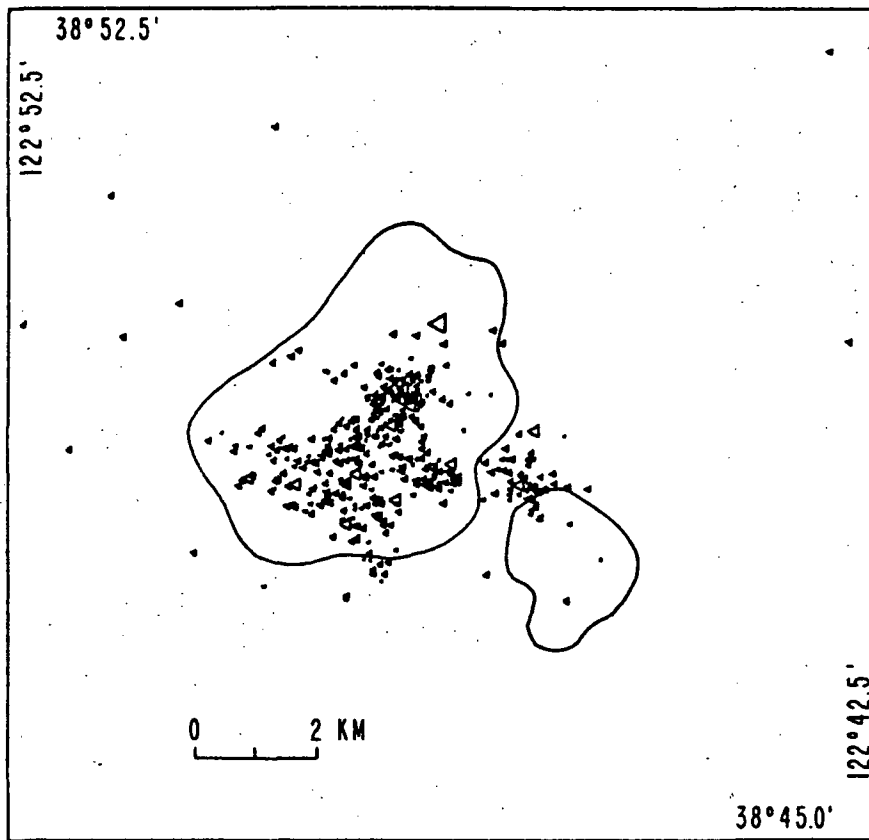
3-D.



THE GEYSERS NOVEMBER 1976 - APRIL 1977

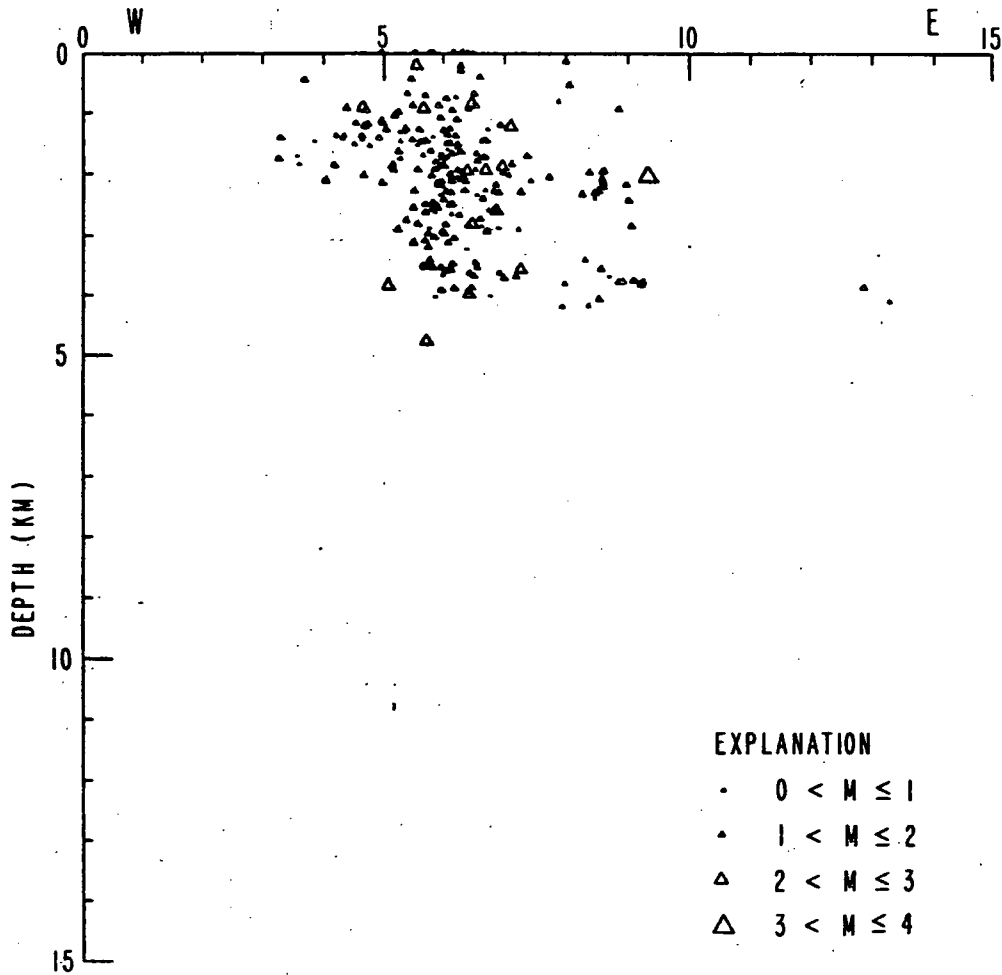
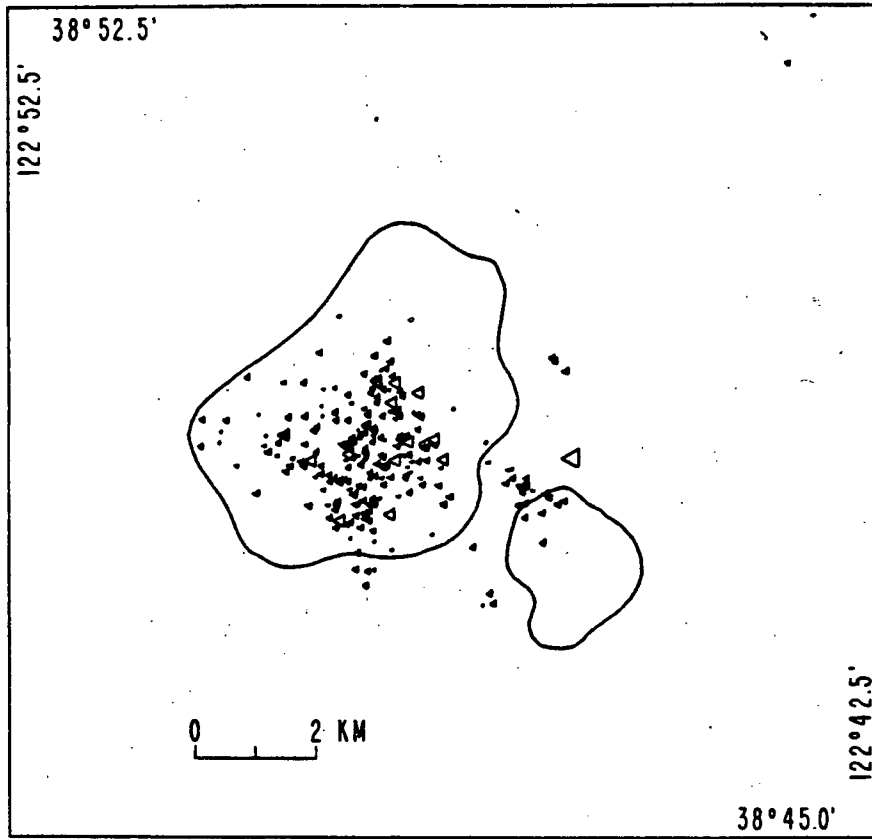
15

3-E.



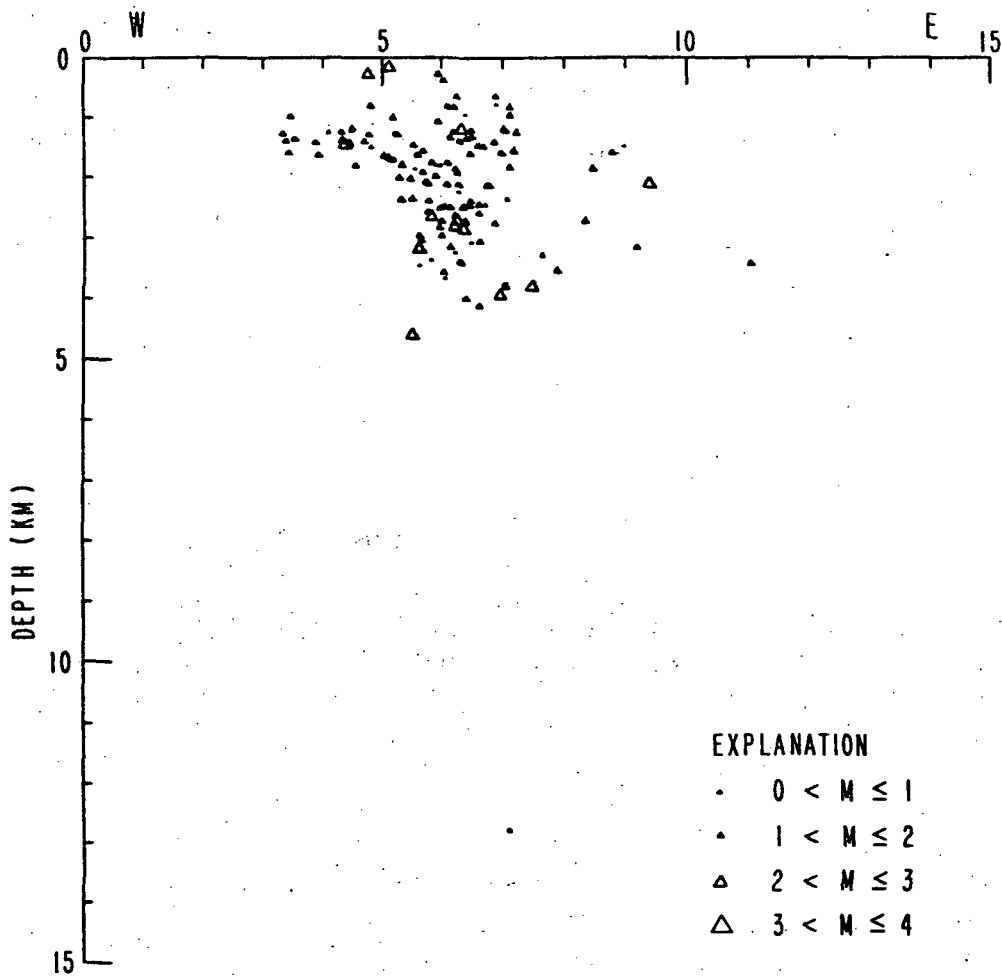
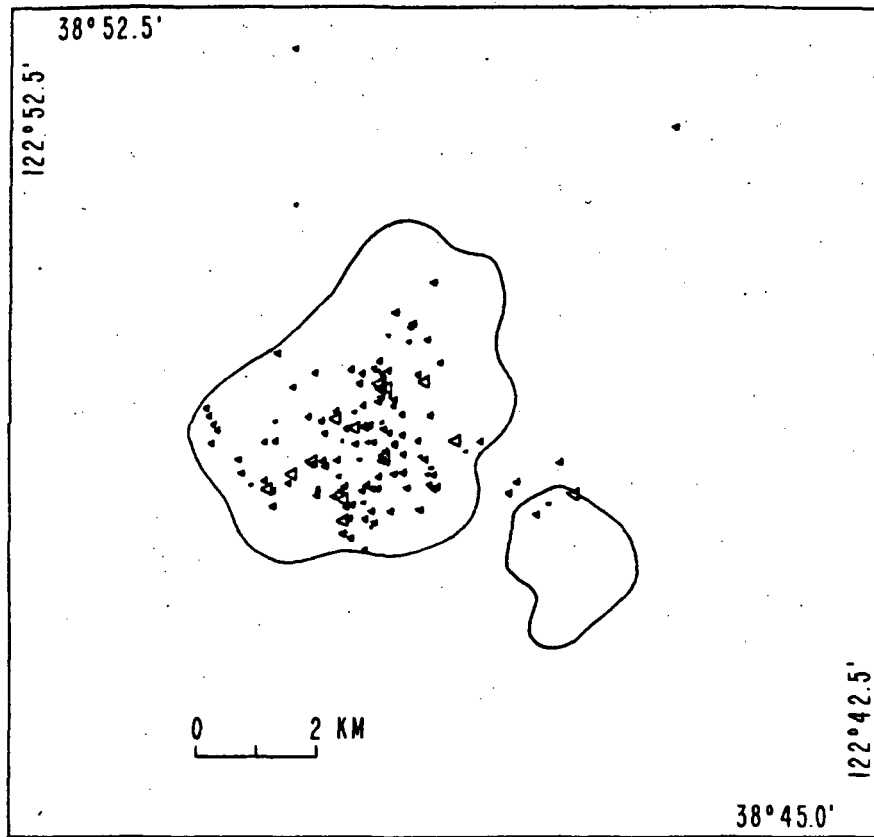
THE GEYSERS MAY 1977 - OCTOBER 1977

3-F.



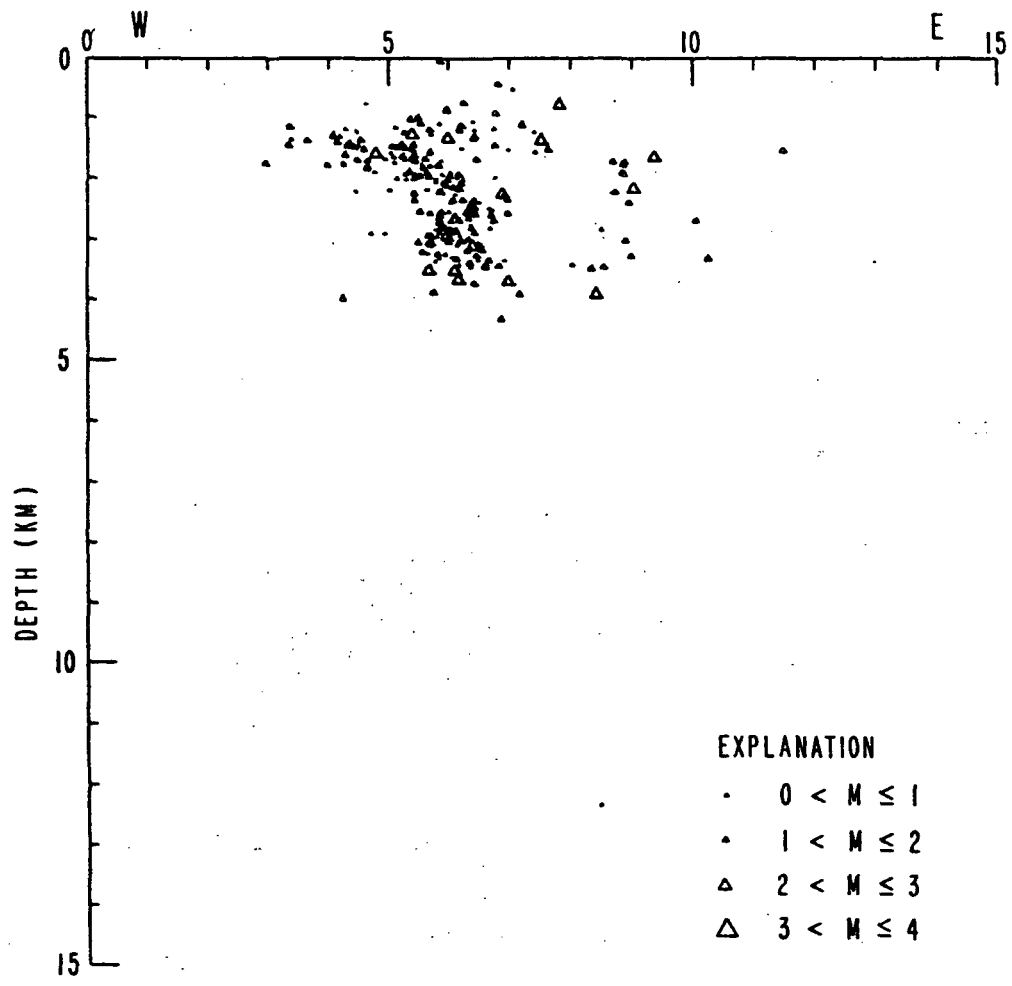
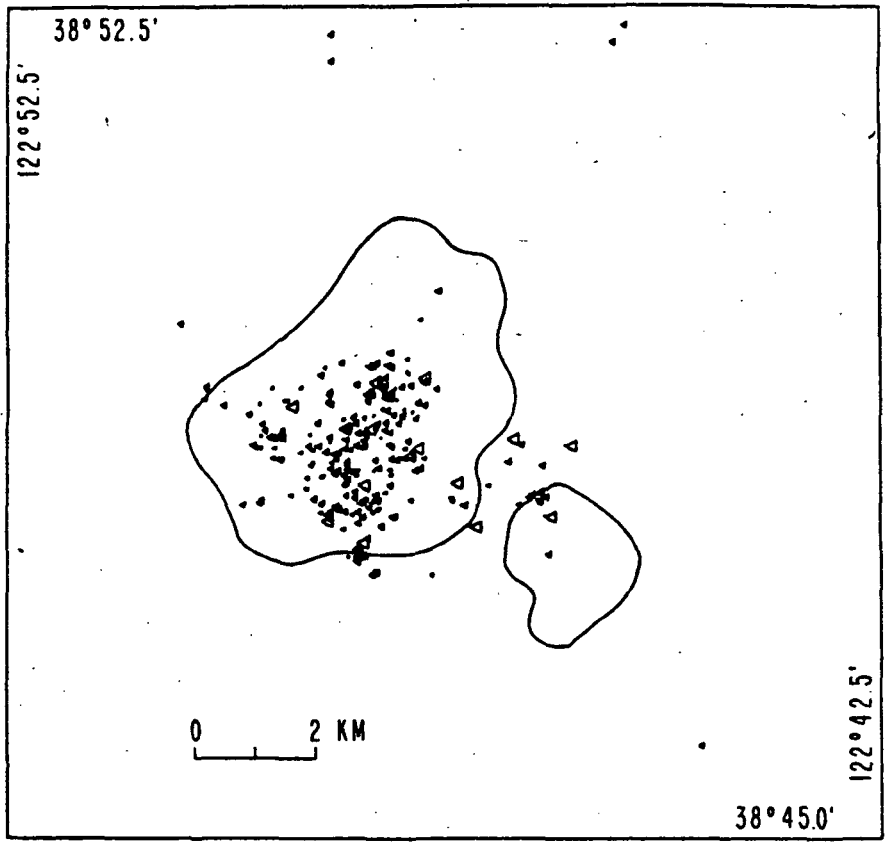
THE GEYSERS NOVEMBER 1977 - APRIL 1978

3-G.



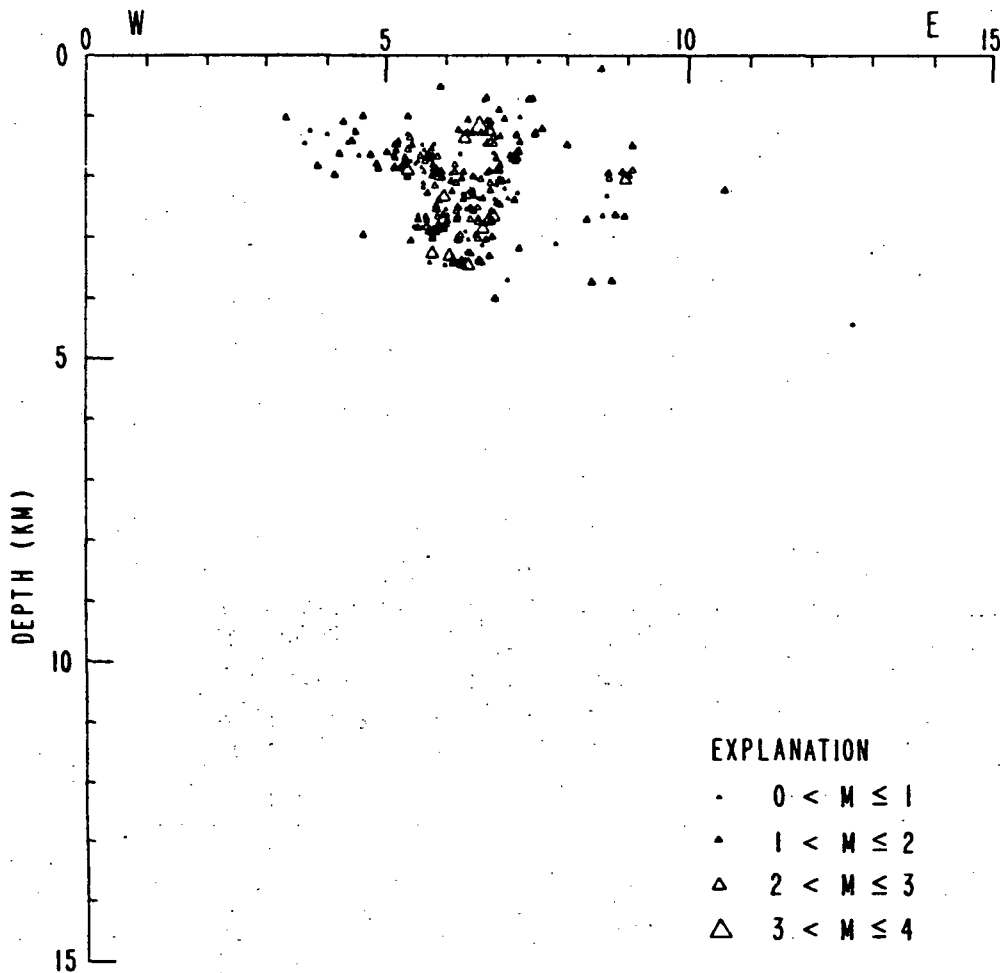
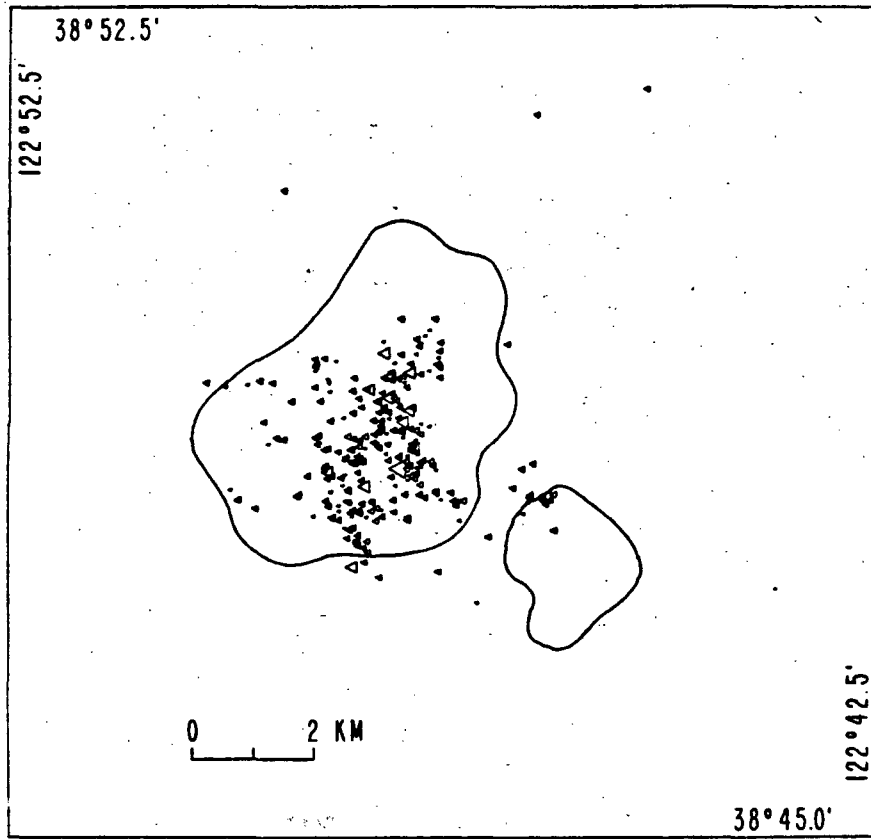
THE GEYSERS MAY 1978 - OCTOBER 1978

3-B.



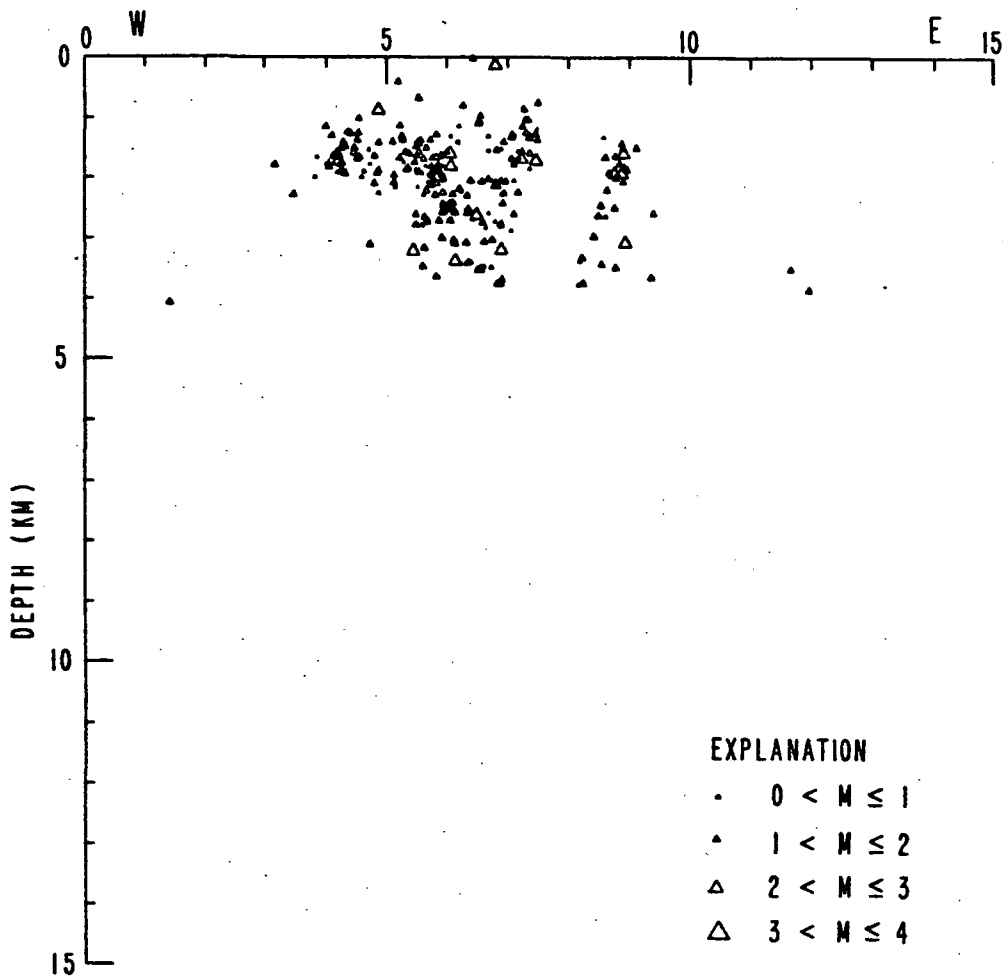
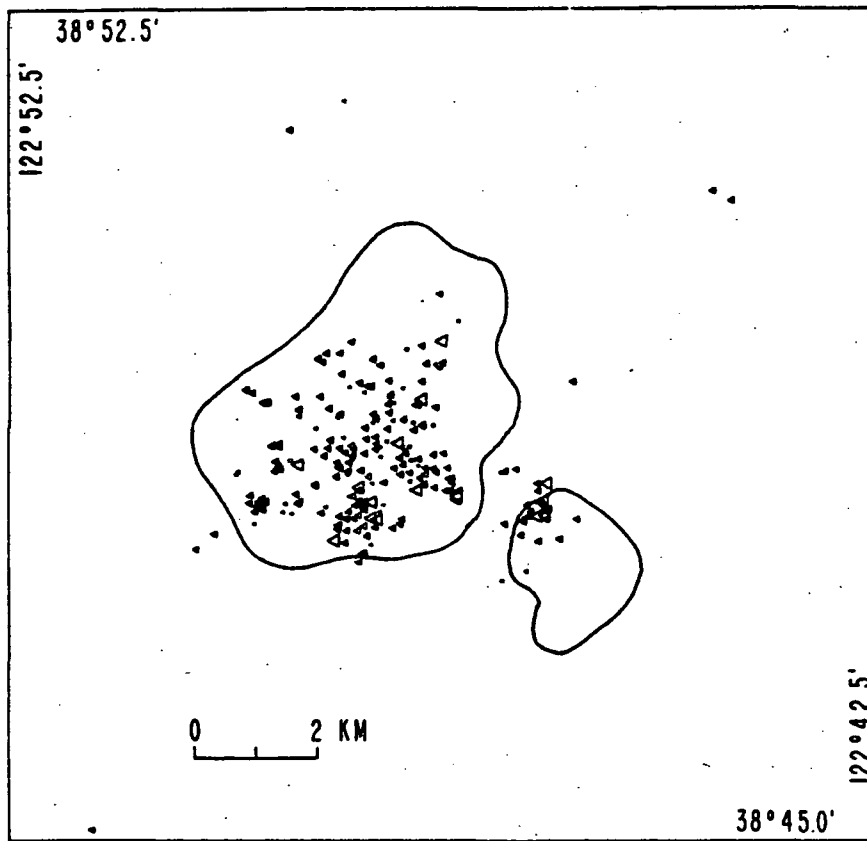
THE GEYSERS NOVEMBER 1978 — APRIL 1979

3-I.



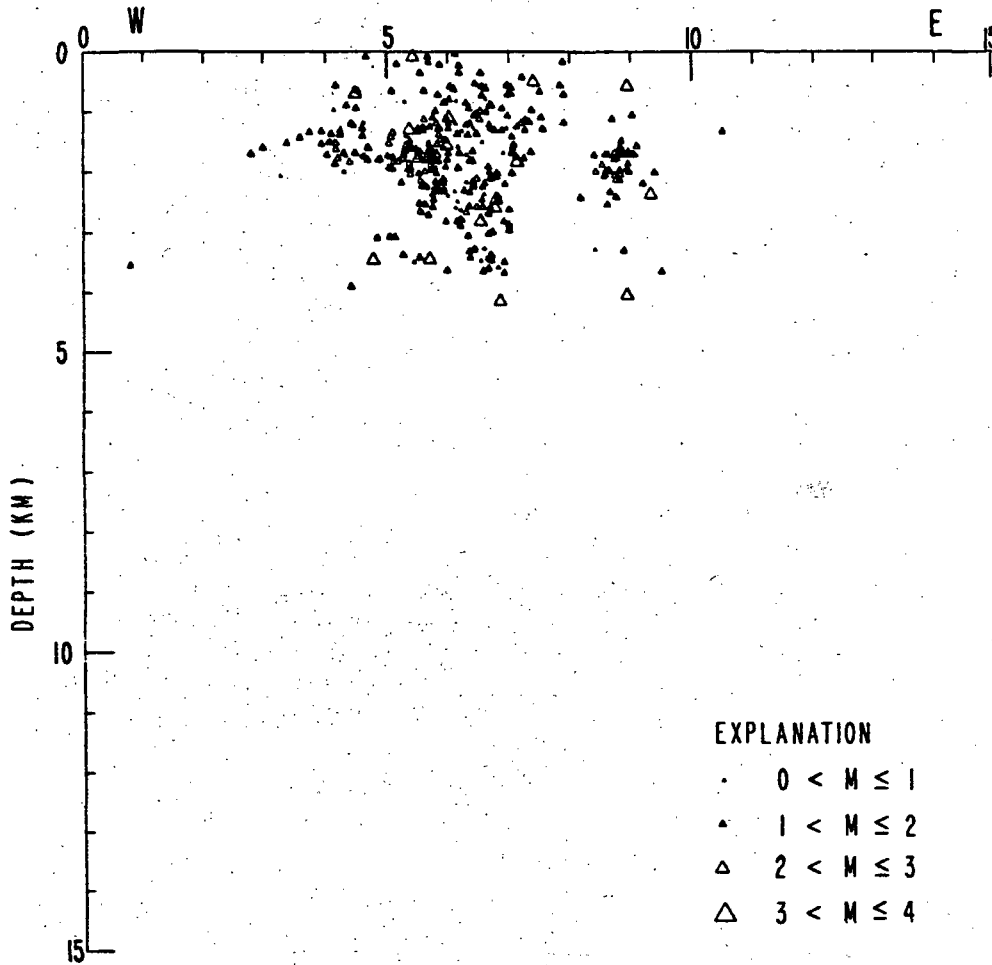
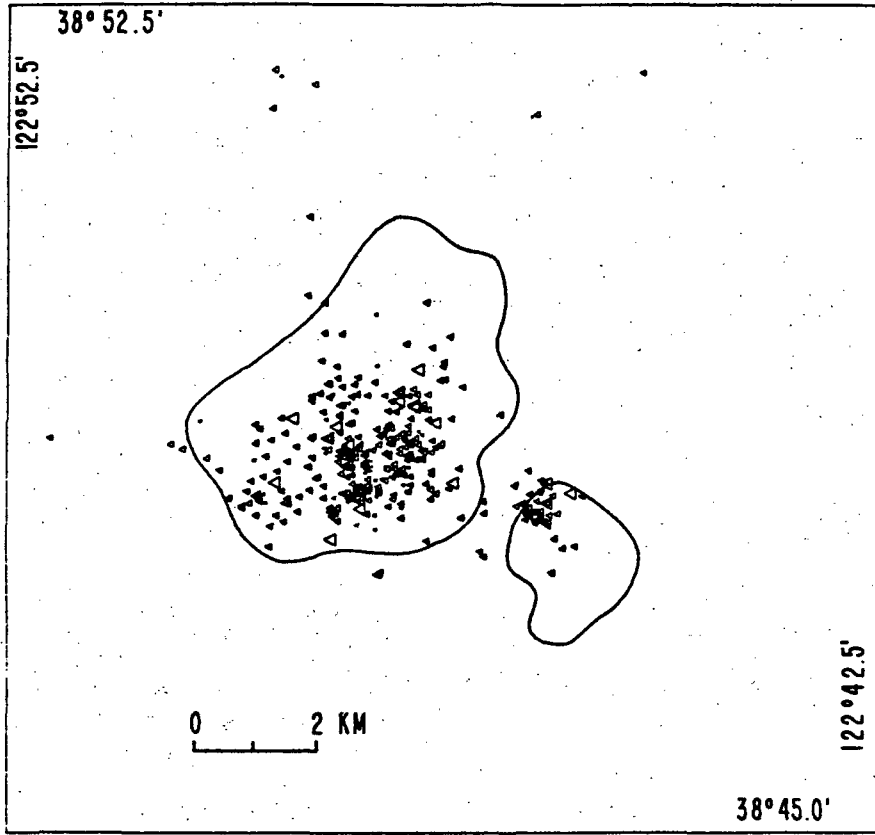
THE GEYSERS MAY 1979 - OCTOBER 1979

3-J.



THE GEYSERS NOVEMBER 1979 - APRIL 1980

3-K.





of events and separation of the two areas of pressure decrease may be due to unfractured and impermeable rock separating two more fractured, permeable rock bodies where events occur. Essentially all of the formation permeability is through the fractures. Although the graywacke with 1% intrinsic porosity (Denlinger, 1979) is almost impermeable, having helium and air permeabilities less than 1 md, as a whole the reservoir has a porosity of 3-7% due to fractures (Lipman et al., 1978). No production or injection wells extend into the aseismic zone, again suggesting an impermeable barrier.

Power production at Plant 15 began in June of 1979. A few earthquakes had been located in the area near Plant 15 (see figure 2) prior to that time, including a temporal cluster of five events in November, 1977. Figure 3J shows a very tight spatial cluster about half a kilometer north of injection well PEC A-6. These events are tightly grouped in space, having a mean depth of 1.7 km with a standard deviation of 0.15 km, but are not clustered in time. Activity began on June 26, within two weeks of the beginning of power production. Earthquake recurrence time varied from several days to several weeks. The spatial cluster is less prominent in the next six-month period (figure 3K), but more events were located in the area surrounding Plant 15 (figure 2) than had been in any of the previous periods.

Also prominent in figure 3K are two dense spatial clusters immediately southeast of two injection wells at which injection began in November 1978 (HJ-9) and March 1979 (GDC 53-13). The rates and history of injection are unknown. Like the events near PEC A-6 in figure 3-J, these spatial clusters are composed of single events occurring days or weeks apart. These events have mean depths of 1.7 km (HJ-9) and 1.6 km (GDC 53-13) with standard deviations

of 0.6 and 0.5, respectively. These injection wells are located near production wells in the most seismically active part of the steam field. For The Geysers as a whole, the mean depth is 2.2 km with a standard deviation of 0.8 km. No unusual activity has been noted near well LF-23 which also began injection in 1979.

Several other features of the seismicity deserve mention. Events in the western part of the field are generally shallower than in the center, with most of the events occurring at depths less than 2 km. North of The Geysers intermittent activity has occurred, (figure 3) with the largest cluster of events occurring in 1975 at Rabbit Valley, 5 km north of The Geysers. Hypocentral locations at The Geysers with improved depth control, since installation of station GDX in November 1977, confirm the absence of seismic activity deeper than 5 km. (Hamilton and Muffler, 1972, Marks et al., 1977, and Majer and McEvelly, 1979). Events located by the USGS California network with  $M_c \geq 1.2$  (completeness level since May 1975) have a mean daily occurrence rate of 0.73 with a standard deviation of 1.01 (May 1975-Dec 1978).

Majer and McEvelly (1979) operated a portable network of 12 stations at The Geysers September 20-24, 1976 and a single station for ten days in 1977. They estimated that twenty-five to thirty events of  $0 \leq M_L \leq 2$  (where  $M_L$  is equivalent to local Richter magnitude) occur daily at The Geysers. Forty events located by Majer and McEvelly in September 1976 are plotted in figure 4 for comparison to USGS data. Our data contradict their reported lack of events in the older steam-producing area serving Units 1 & 2, and indicate that the older area is as seismically active as other parts of the steam production area. A lack of foci between 2 and 3 km of depth, reported by

THE GEYSERS: MAJER AND McEVILLY'S DATA

24

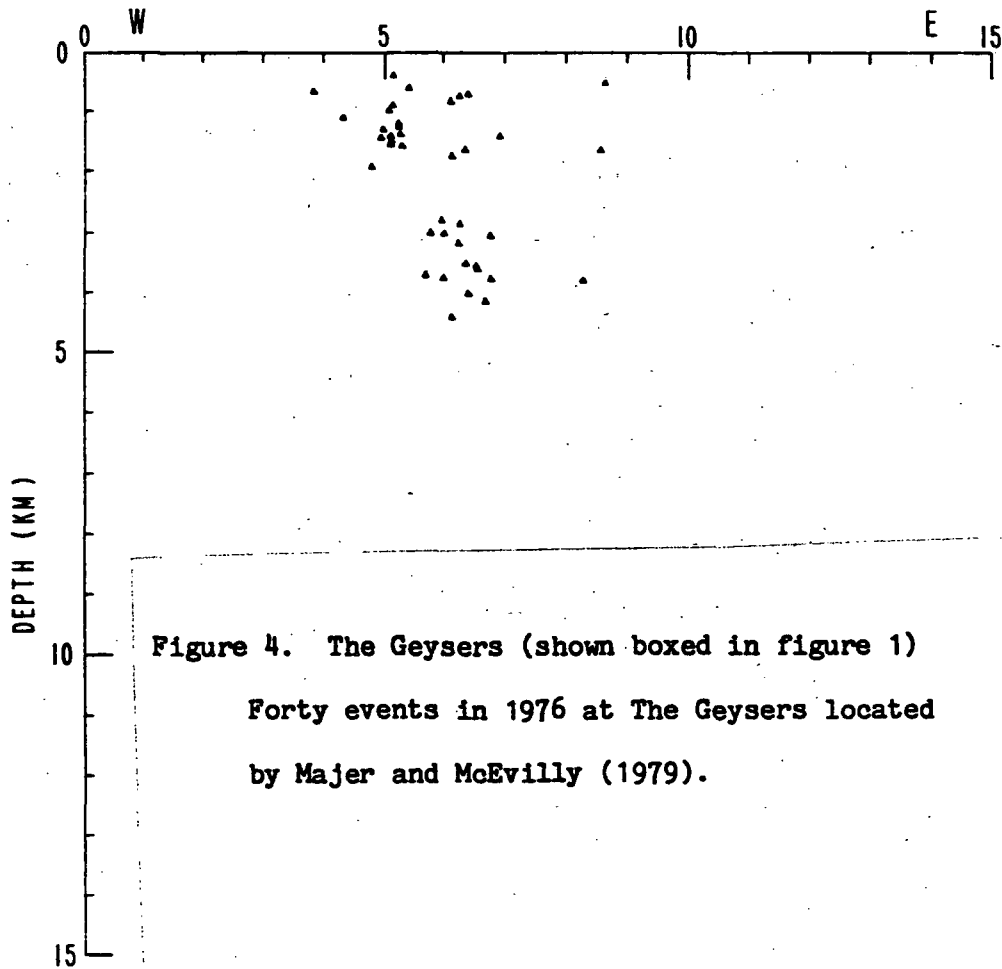
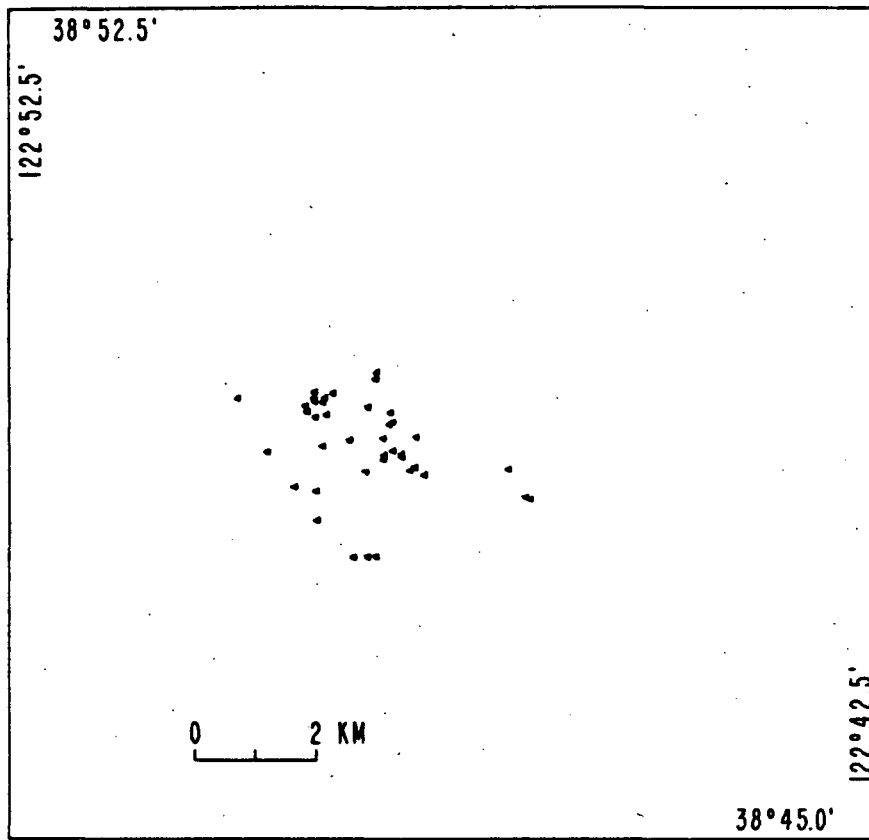


Figure 4. The Geysers (shown boxed in figure 1)  
Forty events in 1976 at The Geysers located  
by Majer and McEvilly (1979).

THE GEYSERS 11/77-12/78

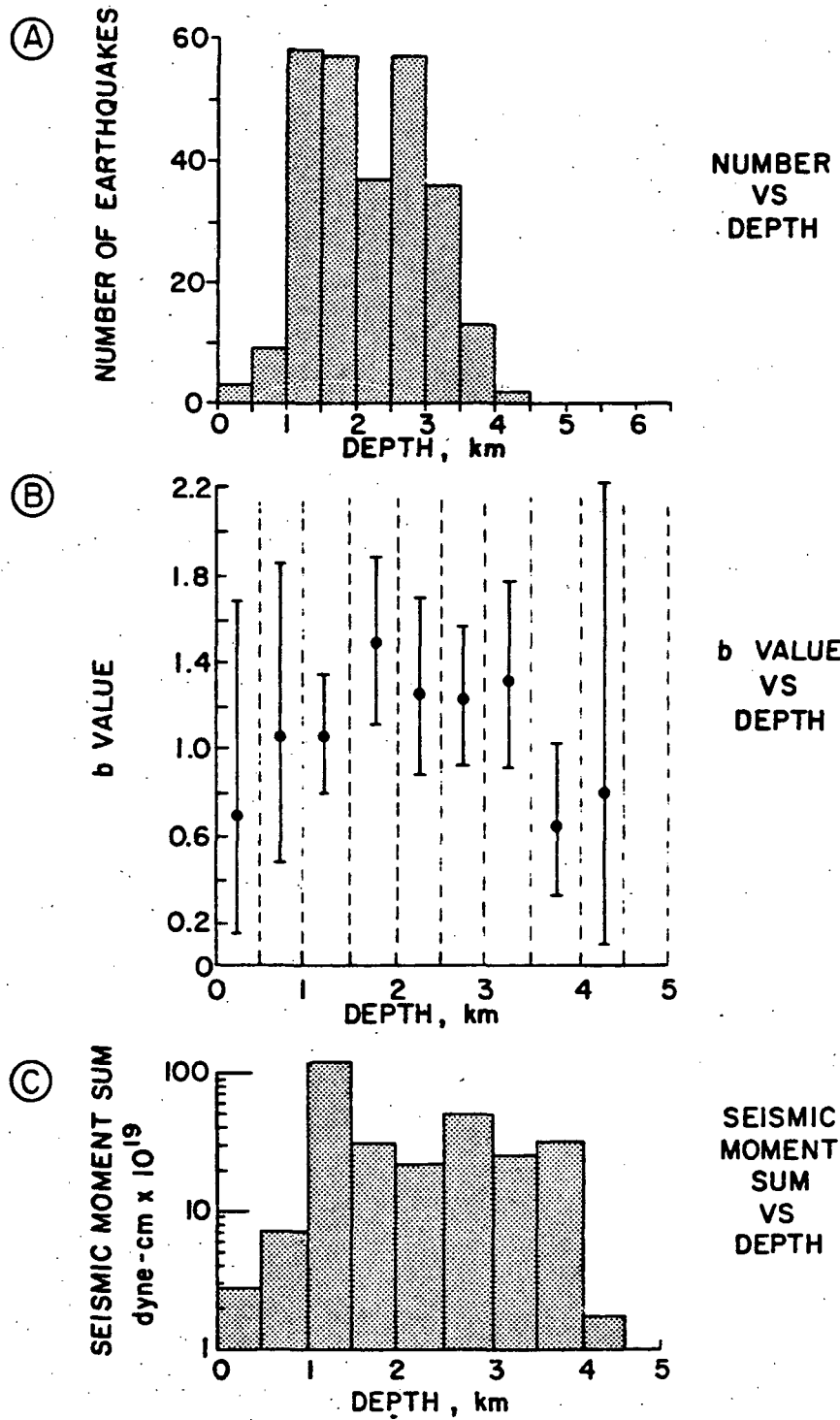


Figure 5. Depth distribution of number of events, b values and seismic moment sums for The Geysers (shown boxed in figure 1) 11/77-12/78.

- (A) Number of events vs. depth
- (B) b value vs. depth
- (C) seismic moment sum vs. depth.

Majer and McEvilly (1979), is less prominent in the USGS data. Figure 5 shows number of events, b values, and cumulative seismic moments as functions of focal depth. Data used for figure 5 were preliminary California Network solutions for events of  $M_c \geq 1.1$  from 11/77 to 12/78, with RMS P-wave travel-time residuals less than 0.30 sec, A and B quality solutions, and distance to the nearest station less than 4 km. Less activity occurred in the 2.0-2.5 km depth range than in the 1.5-2.0 or 2.5-3.0 km ranges. When only events of  $M_c \geq 1.5$  are plotted, the depth distribution is no longer bimodal. Moreover, the moment sum in figure 5 shows no decrease between 2.0 and 2.5 km. This indicates that a depth gap may exist for smaller events.

Alternatively, Majer and McEvilly's gap could be due to normal fluctuations in activity since the time period (5 days) during which they recorded events was brief. Brevity of recording period could also explain the apparent lack of seismicity near Units 1 & 2 in their data. Their model consisted of two layers over a half-space, with velocities of 4, 5, and 6 km/sec and layer thickness of 1 and 5 km respectively. The model used by the U.S.G.S. California network is a 4 km/sec layer with variable thickness over a 5.9 km layer which extends to 15 km depth.

An improved model for The Geysers was obtained by utilizing the inversion program "HYPOINV" of W. Gawthrop (unpublished manuscript). This program solves for a linear increase of velocity with depth over a constant velocity half space. Values obtained for The Geysers region are:  $V_0$  = surface velocity of 4.32 km/sec., velocity increases at 0.21 km/sec per km down to 4.88 km, below which the velocity is 5.73 km/sec. Relocated events of  $M_c \geq 2.5$  from May 1975 - 1978 are shown in figure 6 with fault plane solutions for some events.

RMS travel-time residuals from the improved velocity model were an average of 0.08 seconds smaller than residuals from the California Network model. Table 2 lists times, epicentral locations, depths, magnitudes and RMS P-wave travel time residuals of events shown in figure 6. The California Network coda length-magnitude relation was used. Sixty percent of all events of  $M_c \geq 2.5$  occur in October, November, December, and January; with thirty percent in December. With the exception of December 1977, there has been a large event in December of each year since 1972. The largest number of  $M_c \geq 2.5$  earthquakes in a single month occurred in December 1976 (3 events).

#### Fault Plane Solutions

Fault plane solutions for some of the earthquakes,  $M_c \geq 2.5$ , indicate strike-slip, normal, and thrust faulting, although strike-slip mechanisms predominate. Maximum horizontal compression, obtained from solutions for strike-slip events with fault planes dipping less than 30 degrees, is N. 26 degrees E. , with minimum horizontal compression N. 68 degrees W. The standard deviation is 19 degrees. Analysis of focal mechanisms of earthquakes at The Geysers, along the Maacama fault to the south, and in the Clear Lake Volcanics to the north (Marks et al, 1978) shows that horizontal principal stress orientations at The Geysers are the same as those in the surrounding region. The mechanisms of these earthquakes (figure 6) do not show any clear spatial pattern. Events showing thrust, strike slip, and normal faulting mechanisms may be found within a few hundred meters. This suggests that the stress field is extremely heterogeneous. Amplitudes of horizontal stresses

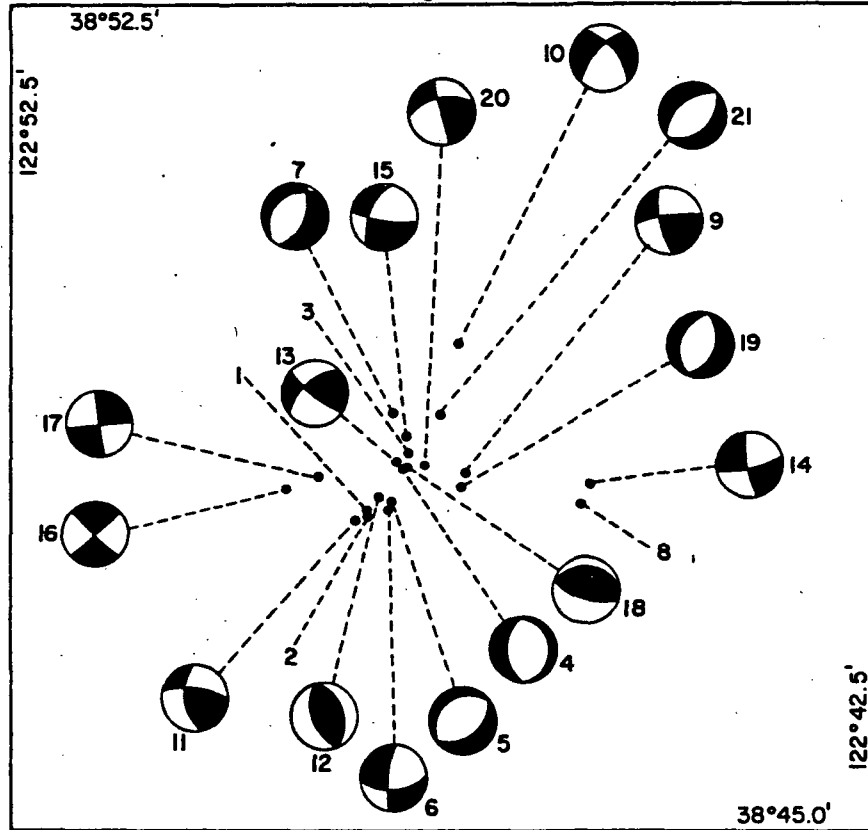


Figure 6. Map view showing locations of events of  $M_c \geq 2.5$  at The Geysers.

Lower hemisphere fault plane solutions for selected events are shown.

Dark areas represent compression. Dates, locations, depths, and P-wave RMS residuals are given in table 2.

Table 2

	DATE/TIME			LOCATION		DEPTH	MAG	RMS
	<u>yr/mo/day/hr/min/sec</u>			lat.	long.	<u>Km</u>	<u>Mc</u>	<u>P-wave</u>
				<u>deg. min.</u>	<u>deg. min.</u>			<u>sec.</u>
1)	751004	1903	24.11	38N 47.92	122W 48.33	4.0	2.8	0.07
2)	751004	1903	41.75	38 47.87	122 48.31	3.8	2.6	0.10
3)	751214	2235	54.57	38 48.44	122 47.84	0.0	2.6	0.13
4)	760118	1925	59.26	38 48.30	122 47.89	1.2	2.7	0.05
5)	760306	1351	08.33	38 48.00	122 48.03	2.2	2.7	0.06
6)	760415	0908	39.25	38 47.91	122 48.07	2.6	2.7	0.04
7)	760512	1418	09.58	38 48.81	122 48.02	4.0	2.5	0.06
8)	760806	2217	54.79	38 47.97	122 45.88	3.8	2.6	0.06
9)	761217	2136	25.57	38 48.26	122 47.19	1.8	2.9	0.06
10)	761222	0042	18.79	38 49.43	122 47.28	2.2	3.1	0.07
11)	761223	0123	53.69	38 47.82	122 48.46	3.7	3.0	0.06
12)	770210	1918	51.65	38 48.05	122 48.20	2.7	2.7	0.06
13)	770724	2138	29.69	38 48.37	122 48.00	1.4	2.6	0.07
14)	770922	2048	42.94	38 48.15	122 45.78	2.7	3.2	0.06
15)	771002	1951	53.59	38 48.50	122 47.86	2.1	2.4	0.06
16)	771128	2236	26.09	38 48.10	122 48.24	1.7	2.5	0.04
17)	780114	0232	48.37	38 48.22	122 48.89	2.0	2.5	0.08
18)	780114	1545	45.33	38 48.31	122 47.86	2.0	2.7	0.06
19)	780715	1457	2.06	38 48.13	122 47.25	1.7	2.7	0.05
20)	781209	1602	27.47	38 48.30	122 47.66	1.3	3.0	0.05
21)	781215	0301	20.68	38 48.79	122 47.47	3.8	2.7	0.05



may vary with time and focal depth (Bufe et al., in press). Events below 2 km at The Geysers have shown temporal swings from strike-slip to normal faulting. This behavior appears to correlate with temporal changes in the regional NE-SW compressive stress, making The Geysers a "stress barometer" for the region (Bufe et al., in press).

### Stress Drops

In theory it is possible to determine the reduction in stress or "stress drop" ( $\Delta \sigma$ ) which occurs during an earthquake from its shear wave moment and corner frequency (Brune, 1970, 1971). This theory has been extended to P-wave spectra by Hanks and Wyss (1972). Peppin and Bufe (1980) found stress drops ranging from 1 to 10 bars for earthquakes in the magnitude 1 to 3 range at The Geysers and surrounding region. On December 9, 1978 at 1602 UT an event of coda magnitude 3.12 ( $M_L = 3.4$ ) occurred near the center of the steam field; one of the largest earthquakes recorded at The Geysers to date. This strike-slip event (number 20 in figure 6) had a depth of 1.3 km, and an epicenter located about 2.9 km from a three component digital event recorder which provided data for spectral analysis. The following information was obtained from spectral analysis:

Component	Seismic Moment	Corner Frequency Hz	Source radius m	Slip cm	Stress Drop bars
		<u>fo</u>	<u>r</u>		
P	$8 \times 10^{19}$ dyne-cm	20.	85.	1.8	57.
S-H	$8 \times 10^{21}$ dyne-cm	1.5	670.	2.8	12.
S-V	$2 \times 10^{21}$ dyne-cm	4.	270.	5.1	56.

The slip and stress drop estimates are fairly consistent, given the large variation in moment and source radius. While the exact relation between stress drop and total shear stress is not known, the above data indicate shear stresses in the steam field can exceed 50 bars.

### Moments

Seismic moment  $M_0$  is the product of elastic modulus, average fault displacement, and fault area. Moments have been determined by spectral analysis for several earthquakes at The Geysers using P and S data from 3-component digital event recorders and P data from vertical component telemetered stations. Most of the moment data are from the University of Nevada array of event recorders deployed at Alexander Valley, 10 km south of the The Geysers, in late November and early December, 1977, (Peppin and Bufe, 1980). The resulting P and S moment data are plotted in figure 7 as a function of the coda magnitude ( $M_c$ ) determined by the central California network. Peppin and Bufe (1980) have shown that  $M_c$  and  $M_L$  do not systematically differ in the magnitude range 1.0 to 2.5 at The Geysers. The magnitude-moment relation for P is well determined at  $\log M_0 = 1.3 M_c + 16.7$ . The relation between  $M_c$  and S moment is less well determined. The locally ( $\Delta = 2$  Km) determined shear moments for Geysers earthquakes are systematically higher than those determined from the recorders at Alexander Valley ( $\Delta = 10$  Km). The data of Peppin and Bufe (1980) also show that

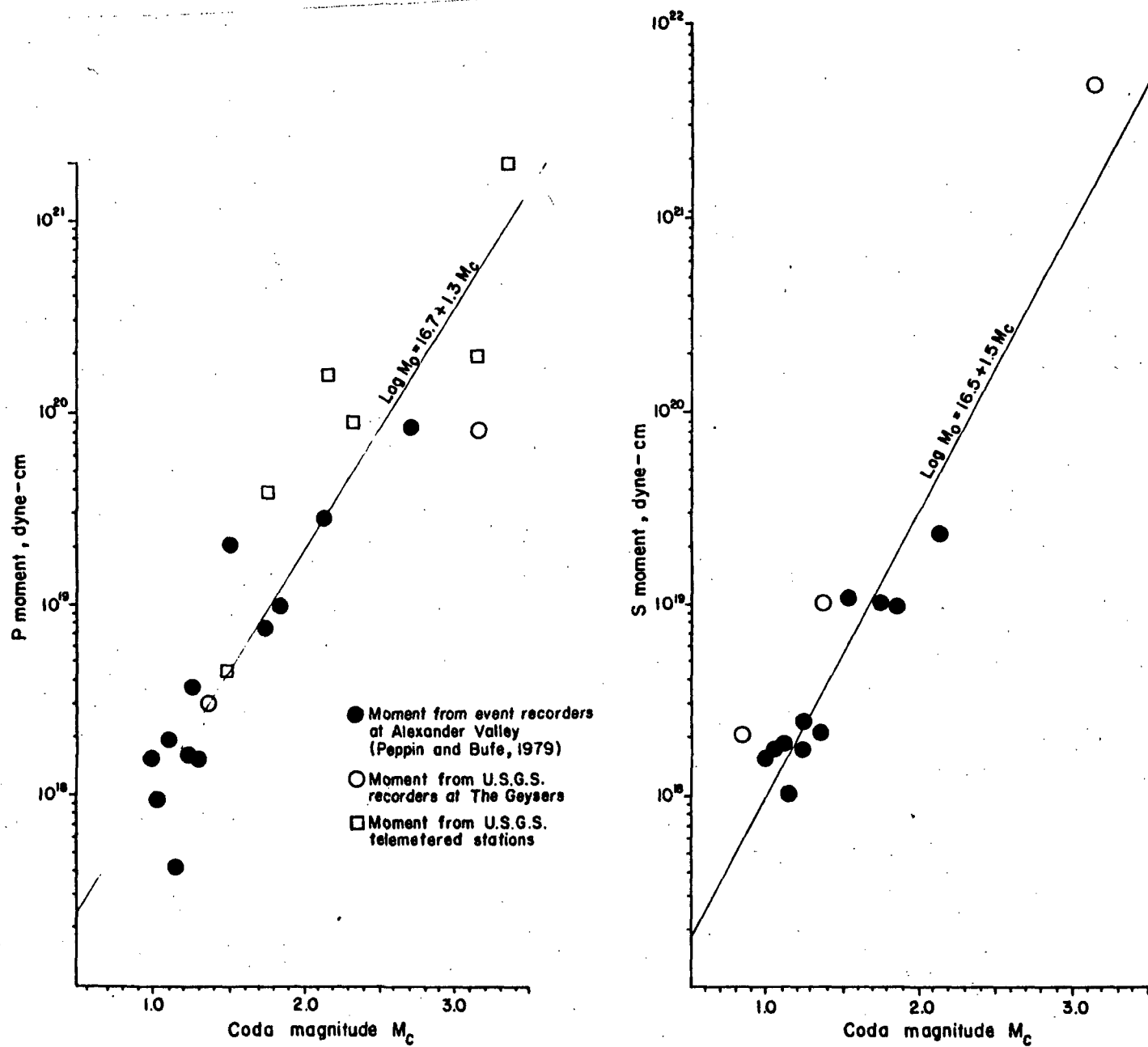


Figure 7. P and S wave moment-magnitude relations for events occurring at The Geysers.

earthquakes near the recorders at Alexander Valley appear to have larger moments than the more distant earthquakes at The Geysers. A moment sum using the S wave moment-magnitude relationship ( $\log M_o = 1.5 M_c + 16.5$ ) obtained for events at The Geysers of  $M_c \geq 1.1$  from May, 1975 to April, 1980 yielded a moment rate of  $6.3 \times 10^{21}$  dyne-cm/year.

Alternatively, the S-wave moment-magnitude relation may be used in combination with the  $\log N = a - bM_c$  relation (where N is the number of events per year), and a stress-drop-moment relation given by Brune (1970, 1971) to estimate moment rate. Using data from May, 1975 to April, 1980 the relation

$$\log N = 3.9 - 1.2 M_c \quad (1)$$

was obtained. Shear moment at The Geysers is given empirically by

$$\log M_o = 1.5 M_c + 16.5 \quad (2)$$

Thus, equations (1) and (2) become

$$\log N = 17.1 - 0.8 \log M_o \quad (3)$$

Therefore;

$$N = 10^{17.1} \times M_o^{-0.8}$$

the moment sum per year is then:

$$\int_0^{\max M_o} N \, dM_o = \int_0^{\max M_o} 10^{17.1} \times M_o^{-0.8} \, dM_o = 5 \times 10^{17.1} M_o^{0.2} \Big|_0^{\max M_o}$$

where  $\max M_o$  is the maximum moment.

In order to compare this estimate to the observed moment sum, only events of  $M_c \geq 1.1$  may be considered. Using the magnitude-moment relation, an event of  $M_c = 1.1$  has a shear wave moment of  $1.4 \times 10^{18}$  dyne-cm. Therefore, the lower limit of integration is  $1.4 \times 10^{18}$  dyne-cm.

Next, an upper limit of integration, representing the moment of a maximum seismic event ( $\text{Max}M_o$ ) must be defined. Since seismic moment,  $M_o$ , is defined as  $\mu \bar{u} A$ ; where  $\mu$  is the shear modulus,  $A$  is the area of the fault, and  $\bar{u}$  is the average displacement over the fault; an estimate of  $\text{max}M_o$  can be calculated for a rupture tearing completely through the producing reservoir and existing seismic area. First, fault area is maximized by assuming a fault the length of the seismic area (6 km) which extends to the maximum depth of seismic activity (4 km). This is equivalent in area to a circular zone of radius 2.76 km. Maximum moment may now be estimated by assuming that the stress drop ( $\Delta \sigma$ ) is the same as that observed for the Dec. 9, 1978 event and using the relation

$$\bar{u} = \frac{\Delta \sigma}{\mu} r \frac{16}{7\pi} \quad (\text{Brune, 1971})$$

rearranging terms;

$$M_o = \frac{16}{7} r^3 \Delta \sigma$$

If  $(\Delta \sigma) = 5 \times 10^7$  dyne/cm (as on Dec. 9, 1978)

and let  $r = 2.76$  km where  $r$  is the radius of a circular fault

surface.

Then the maximum moment ( $\max M_o$ ) is  $2.4 \times 10^{24}$  dyne-cm, and the calculated moment rate is equal to:

$$5 \times 10^{17.1} M_o^{0.2} \left\{ \begin{array}{l} M_o = 2.4 \times 10^{24} \\ = 4.5 \times 10^{22} \text{ dyne-cm/year} \\ M_o = 1.4 \times 10^{18} \end{array} \right.$$

This estimate is a factor of seven higher than the observed moment rate of  $6.3 \times 10^{21}$  dyne-cm/year because the upper limit of the integration represents a maximum event ( $M_o = 5.3$ ) which was absent from our data set. The observed moment rate was computed from only five years worth of data, while estimated recurrence times for large events are much longer (360 years for an event of  $M_o = 5.3$ ). Therefore, since the calculated moment rate provides for the occurrence of events larger than any yet observed, it may be closer to the actual value of the seismic moment rate.

### Seismic Deformation

The estimates of an average fault displacement in the December 9, 1978 earthquake range from about 2 to 5 cm. Since these are averages over the fault plane, one might expect the displacement to be significantly greater near the center of the slipped area. Thus, displacements on the order of 10 cm may

have occurred. One might expect that this much shearing would have produced noticeable changes in steam flow in nearby wells, but no post-earthquake production difficulties or changes were reported by Union Geothermal.

Using the observed yearly moment rate of  $6.3 \times 10^{11}$  dyne-cm year, recalling that average slip  $= \bar{u} = M_0 / A \mu$ , assuming a value of  $\mu$  of  $2.0 \times 10^{11}$  dyne/cm and using  $24 \text{ km}^2$  as the area;

$$\bar{u} = .131 \text{ cm/year.}$$

This is an order of magnitude less than the surface deformation rates, 3 cm/yr of subsidence and 2 cm/yr of horizontal convergence, observed across the reservoir (Lofgren, in press). Thus, it appears that much of the geodetic deformation occurs aseismically. Large scale inelastic deformation reflected in the geodetic data may concentrate stress in the more competent parts of the field, as suggested by the occasional local occurrence of relatively large seismic displacements like that estimated for the Dec. 9, 1978 earthquake. Alternatively, observed geodetic changes may be due to stress accumulation.

#### Geodetic, Gravity and Reservoir Pressure Changes and Seismic Moment

Studies of the producing area of The Geysers steam field indicate geodetic changes (Lofgren, 1978) on the order of centimeters per year, and gravity changes (Isherwood, 1978) on the order of tenths of a milligal per year. Reservoir pressure studies (Lipman et al., 1978) indicate the existence of two independent pressure sinks, areas of decreased shut-in steam well pressure.

The larger sink has existed since at least 1966 and the smaller since 1975. The pressure sinks have expanded outward as production increased as indicated by contours in figure 3. By April 1977 the pressure decrease was 200-250 psia (pounds per square inch absolute pressure) in the larger, older sink owing to the production for units 1-8 and 11, and 0-50 psia in the smaller sink owing to the production for units 9 and 10. The 500 psia contours of spring 1977 are shown in figures 3E-3K.

Data from a strip 0.8 km on either side of line A-A' as shown in figure 2 (38°49.22' latitude, 122°51.44' longitude to 38°46.30' latitude 122°43.39' longitude) were used to generate profiles in figure 8 of:

- 1). Gravity changes 7/74-2/77 (written communication, W. Isherwood)
- 2). Geodetic changes 1973-1977 (Lofgren, 1978)
- 3). Cumulative Seismic Moment 5/75 - 9/78
- 4). Reservoir Pressure 1977 (Lipman, et al., 1978)

Curves depicting gravity and elevation changes were smoothed by averaging adjacent values. This operation was carried out twice. Moment values were calculated for twenty-four subzones along A-A' using the relation:

$$\log M_0 = 1.3 M_c + 16.7$$

where  $M_0$  = moment and  $M_c$  = coda length magnitude.

Values for reservoir pressure and changes in elevation and gravity are coherent. The largest changes in elevation, gravity and pressure coincide with the peak of the seismic moment sum in the most heavily exploited area of the steam field.

Where the profiles cross the eastern (smaller) pressure sink a flattening of the elevation curve and a second minimum in the smoothed gravity curve are



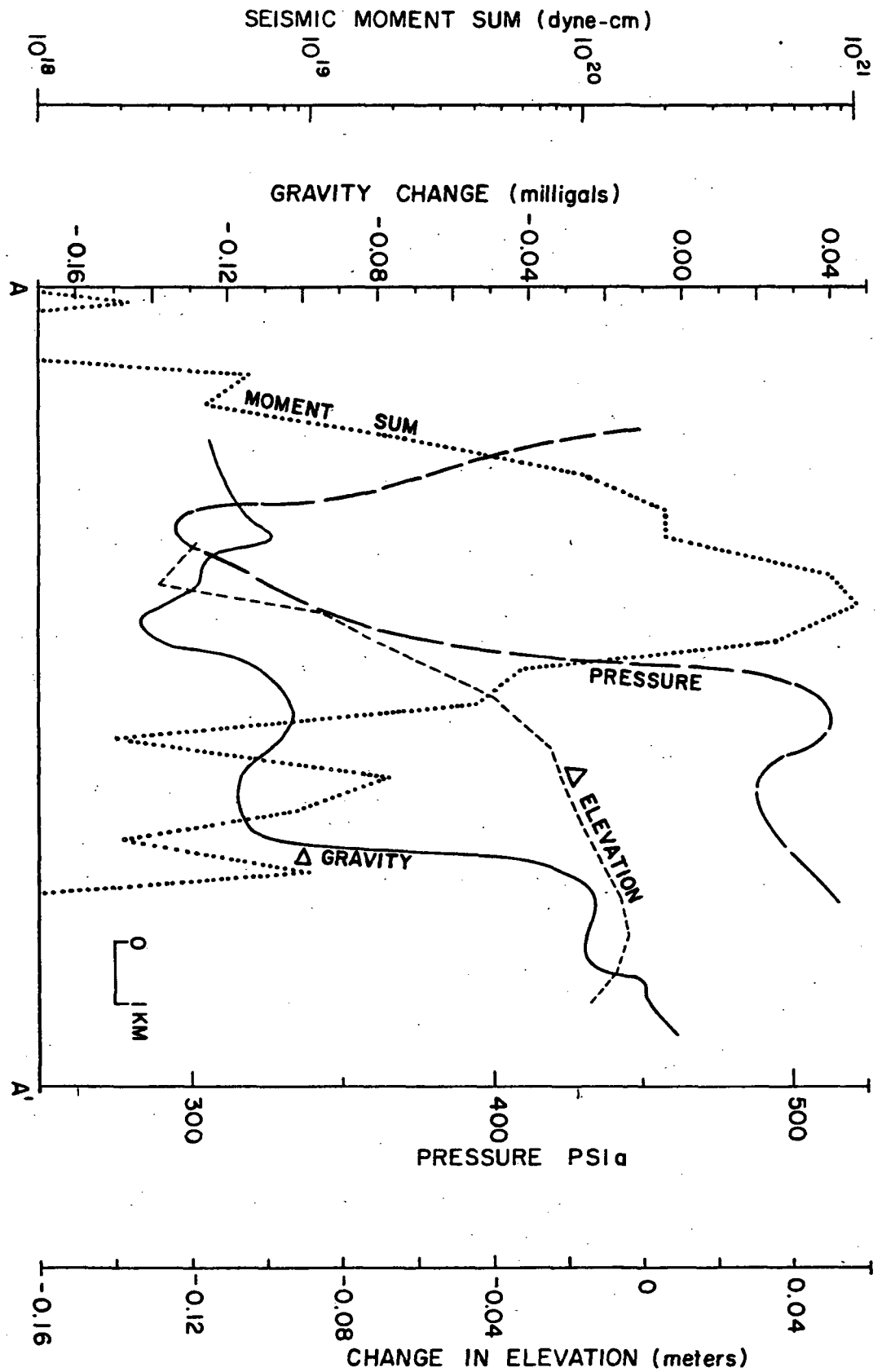


Figure 8. Profiles along line A-A' shown in figure 2. Profiles show gravity changes 7/74 - 2/77, geodetic changes 73-77, cumulative seismic moment 5/75 - 9/78, and reservoir pressure in 1977.

visible. A sizable earthquake cluster occurs near the eastern pressure sink. Most of the larger events lie near an injection well (LF-3) north of the A-A' area, accounting for the relatively low seismic moment in the profile.

### Temporal Variations in Seismicity

In order to determine whether seismic activity at The Geysers shows characteristics similar to regional seismicity, spatial and temporal variations of seismicity in the two boxed areas shown in Figure 1 were compared by statistical analysis.

Data from the U.S. Geological Survey California Network with magnitudes higher than 1.2 were analyzed for The Geysers (38°45', 122°52.50', 38°52.50', 122°42.50') (figures 2-4 and 6) and for the larger area which completely surrounds it called 'Outside The Geysers' (38°33.75', 123°02.50'; 39°03.75', 122°32.50') shown in figure 1. The data set selected is complete at magnitude 1.2 for the time period analyzed, May, 1975 through December, 1978. Mean number of events per day ( $\bar{x}$ ) and variance to mean ratio were computed for discrete samples of two months time for both regions. The variance,  $\sigma^2$ , was calculated by counting; in each 2 month sample, the number of days with zero events, with 1 event, with 2 events, etc.; and applying the standard equation:

$$\sigma^2 = \sum_{j=0}^n (j-\bar{x})^2 P(j)$$

where  $P(j)$  is the probability of  $j$  events occurring in one day. This probability is given by the frequency of occurrence. Results, presented with steam production in

kilograms/hour at The Geysers, are shown in figure 9. Since the area 'Outside The Geysers' is eleven times as large as The Geysers, the difference in the rates of activity in the two areas is even greater than suggested by figure 9. In fact, the rate of activity at The Geysers is approximately 35 times higher than in the surrounding region.

Clustering of events in time may be characterized by the ratio of variance to mean. The Poisson distribution is a stochastic model frequently used to describe seismic activity which consists of random unrelated events. It has a variance to mean ratio of unity. However, swarm activity and mainshock-aftershock sequences are not Poisson processes, since the events are related. A non-random distribution due to events in swarms or mainshock-aftershock sequences will produce a variance to mean ratio exceeding unity. The ratio is dimensionless and independent of area. Figure 9 shows that in the area 'Outside The Geysers', increases in the mean are accompanied by increases in the variance/mean. This indicates that bursts of activity show clustering in time like mainshock-aftershock or swarm sequence. This pattern is not apparent at The Geysers. Although some variance/mean peaks correspond to the regional pattern, the mean number of events/day frequently show negative correlations with the variance by mean ratio, indicating that increases in activity are not generally related to mainshock-aftershock or swarm sequences.

As noted, the rate of activity at The Geysers is much higher than in the surrounding area. Moreover, a six-month periodic oscillation modulates the mean number of events/day, with maxima in January-February and August-September. This semi-annual cycle may coincide with seasonal

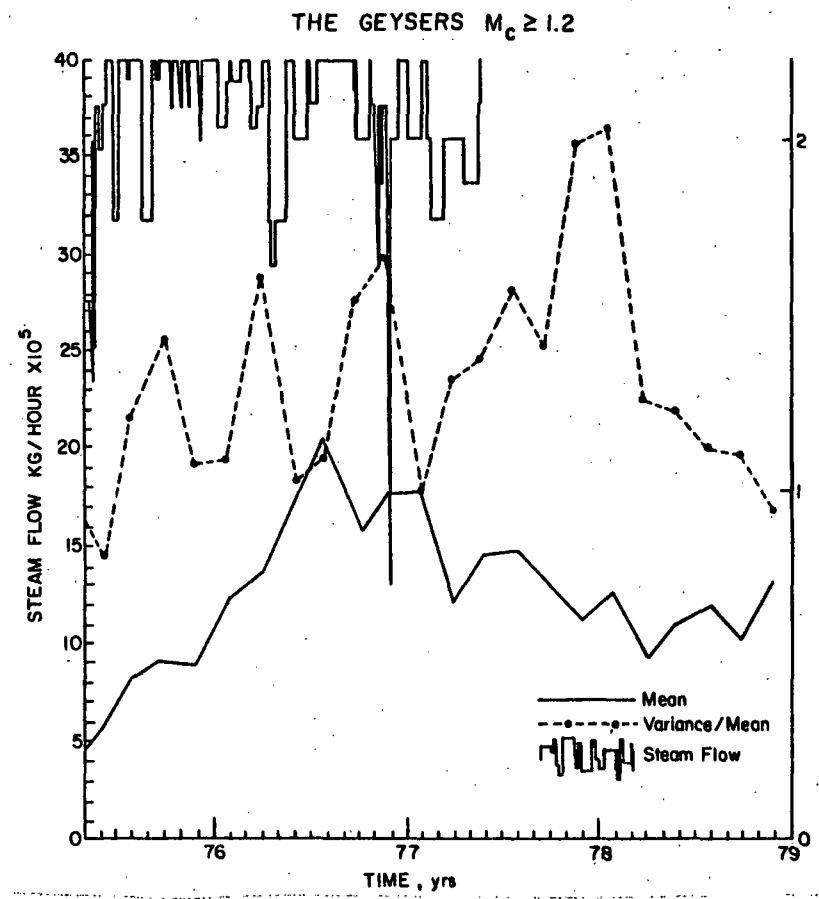
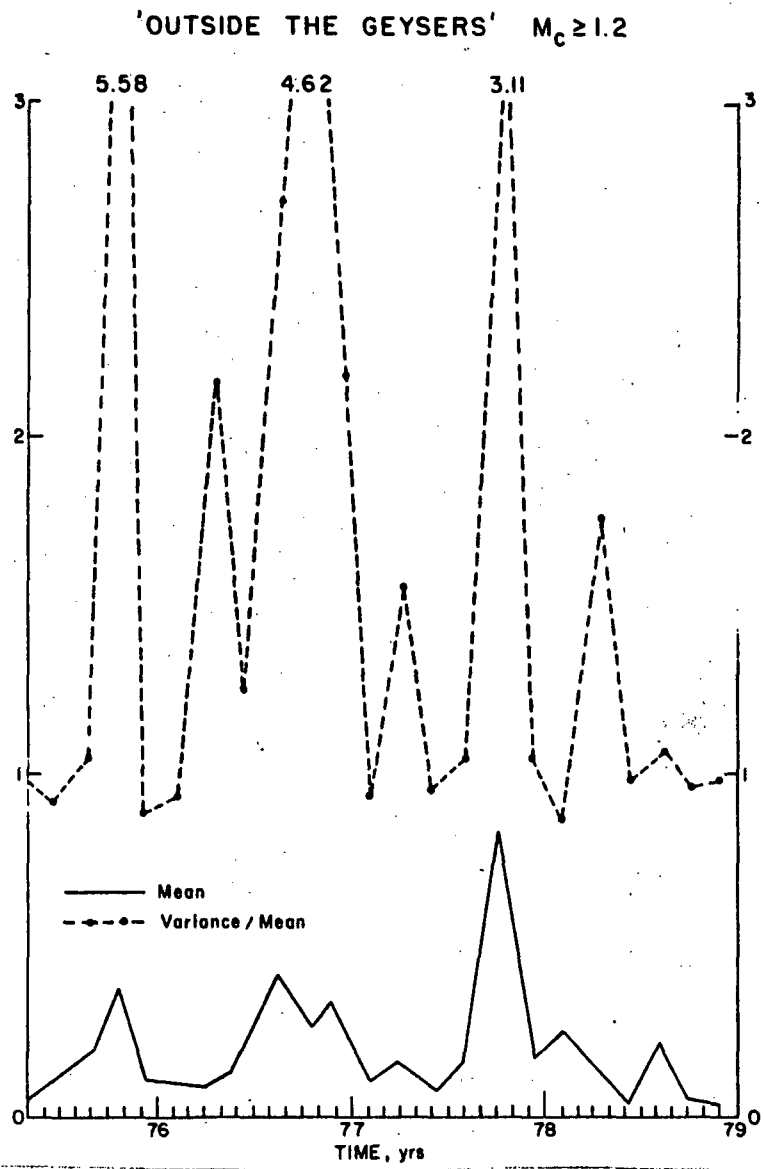


Figure 9. Mean and variance/mean of The Geysers and the area 'Outside The Geysers' (shown in figure 1). The area 'Outside The Geysers' is 11 times as large as the area of The Geysers. Area affects the mean but not the variance/mean. Steam flow used for energy production at The Geysers is shown in kg/hour.

variations in water table levels. The possible existence of other causes for the semi-annual cycle needs further investigation. The January-February and August-September maxima contrast with the peak occurrence of events of  $M_c \geq 2.5$  which is in December, as mentioned earlier.

A striking feature of the mean in The Geysers region is the marked increase of seismicity from May-June 1975, when the seismic data set improves, to July-August 1976, when a maximum of 1.18 events of  $M_c \geq 1.2$  per day is reached. After July-August 1976, the mean shows a decrease until at least December 1978 when the data set ends. Again referring to figure 9, an increase in steam production occurred in May 1975 when power plant 11 began operation at a capacity of 110 Megawatts. This has been the only opportunity thus far to monitor seismic activity contemporaneously with major new production of steam: further opportunities are currently presented by production for plants 12 and 15, which went on line in 1979, and plant 13 which began operating in 1980. Plant 14 is scheduled to begin operation in August 1980 (table 1).

A less detailed history of steam production is shown in figure 10, which only shows increases associated with starting dates for various power plants. Also plotted is the largest event located at The Geysers per year for 1972 through 1978. Wood Anderson magnitudes determined by the Berkeley seismographic station were used. USGS locations were used since Berkeley locations are not well enough constrained to definitively locate events at The Geysers. The USGS located no events at The Geysers prior to 1972. The largest annual event shows a progressively increasing value from 1972-1977 from  $M_L = 3.1$  to  $M_L = 3.8$  which correlates with increases in steam production. A plateau in the level of steam production after May, 1975 precedes a decrease of maximum yearly magnitude in 1978 to  $M_L = 3.4$ .

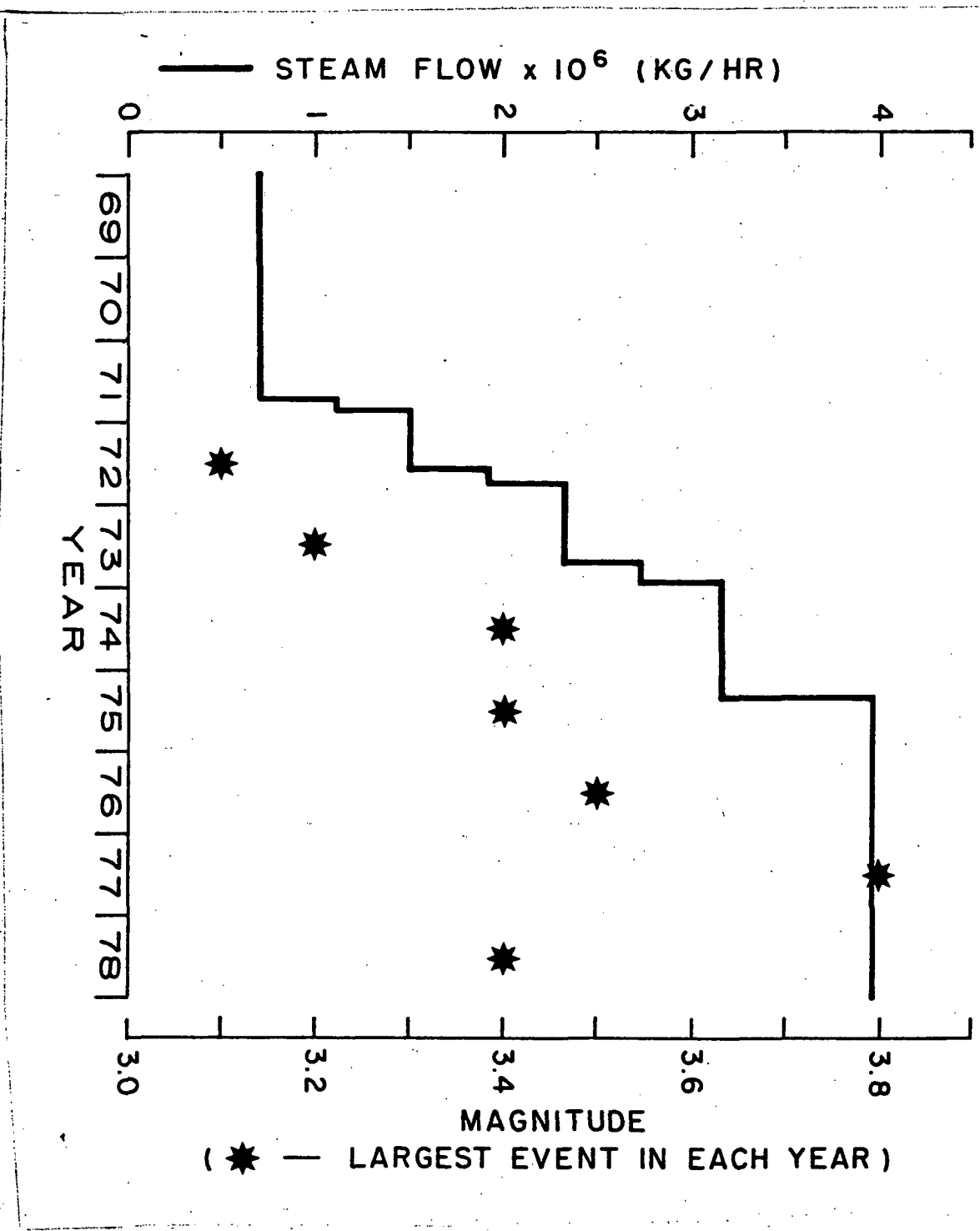


Figure 10. Largest annual events 1972-1978, plotted as asterisks, and steam flow (kg/hour) for the same time period.

## Conclusions

Geothermal development at The Geysers predates the extension of the U.S.G.S. seismic network into the area in 1975. Since 1975 two persistent spatial seismic clusters have been located at The Geysers. The seismic clusters coincide with the most heavily exploited area of the steam field. In this part of the geothermal field steam is produced from a highly fractured graywacke. The fractures, which permit the passage of geothermal fluids through otherwise impermeable rock, also weaken the graywacke. Less stress may be required to trigger seismic events than would be in more competent rock. It is likely that exploitation of the steam field contributes substantially to seismicity in the area by altering effective stress in the fractured rock body. Characteristic fractures which made geothermal development possible may also contribute to the seismicity.

Probable effects of development on Geysers seismicity are shown by the spatial coherence of gravity, pressure, and geodetic changes with seismic moment sums (figure 8); the increase in the mean number of events/day following initiation of steam production for plant 11 in 1975 (figure 9), and the increase in maximum annual Wood-Anderson magnitudes 1972-1977 (figure 10). The increase in maximum magnitude corresponds to increasing steam production, and the decrease in maximum annual magnitude occurred after steam production had been constant for about three years.

The occurrence of the two largest seismic events between 5/75 and 12/78 near the two injection wells most distant from production wells suggests a

link between fluid injection and larger events. It is also notable that peak months for occurrence of large events (October through January) differ from the January-February and July-August biannual maxima seen in the mean numbers/day for all events of  $M_c \geq 1.2$  (figure 9). September to December is the annual period of greatest increase in mean sky cover (sunrise to sunset) and normal monthly total precipitation in northern California (Climatic atlas of the United States, 1968). These factors have a direct effect on the amount of fluid which may be condensed and injected. A rapid increase in amount of injected fluid could, through increased pore pressure and localized cooling, cause changes in effective stress contributing to seismicity. Comparison of spectral analyses of events occurring near injection wells with events elsewhere might distinguish natural from induced events.

Steam production from previously undeveloped and aseismic areas began in 1979 and 1980 (plants 13 and 15). Preliminary data suggest an increase in seismicity near plant 15 shortly after the plant went on-line in 1979. Ongoing seismic studies should further determine the effect of production on seismicity, and could provide a means of distinguishing natural from induced events.



References

- Basili, A., Basili, M., Cagnetti, V., Columbino, A., Jorio, V.M., Mosiello, R., Norrelli, F., Pacilio, N., Polinari, S., 1977, Earthquake Occurrence as Stochastic Event: Theoretical Models, *Revista Italiana di Geofisica*, v. 20, no. 73-74, p. 3-10.
- Brune, J. N., 1970, Tectonic stress and the seismic shear waves from earthquakes, *J. Geophysical Research*, v. 75, p. 4997-5009.
- Brune, J. N., 1971, Correction, *J. Geophysical Research*, v. 76, p. 5002.
- Bufe, C. G., Marks, S. M., Lester, F. W., Ludwin, R. S., Stickney, M. C., in press, Seismicity of The Geysers-Clear Lake geothermal area, California, in McLaughlin, R. J. and Donnelly-Nolan, J. M., eds., *Research in the Geysers-Clear Lake geothermal area*, U.S. Geological Survey Professional Paper 1141.
- Climatic Atlas of the U.S. 1968, U.S. Dept. of Commerce, Environmental Services Administration, Environmental Data Services, 80 pp.
- Denlinger, R., 1979, Geophysics of The Geysers Geothermal Field Northern California, dissertation, Stanford University, 86 pp.

- Hamilton, R. M., and Muffler, L. J. P., 1972, Microearthquakes at The Geysers geothermal area, California, *Journal of Geophysical Research*, v. 77, p. 2081-2086.
- Hanks, T. C., Wyss, M., 1972, Use of body wave spectra in the determination of Body Wave Source Parameters, *Seismological Society of America Bulletin*, v. 62, no. 2, p. 561-590.
- Hearn, B. C., Donnelly, J. M., and Goff, F. E., 1976, Geology and geochronology of the Clear Lake volcanics, California, in *Proceedings, Second United Nations Symposium on the Development and Use of Geothermal Resources*, p. 423-428.
- Iyer, H. M., Oppenheimer, D., Hitchcock, T., 1979, Abnormal P-wave delays in The Geysers-Clear Lake geothermal area, California, *Science*, v. 204, p. 495-497.
- Isherwood, W., 1976, Gravity and magnetic studies of The Geysers-Clear Lake geothermal region, in *Proceedings, Second United Nations Symposium on the Development and Use of Geothermal Resources*, p. 1065-1073.
- Kovach, R. L., Nur, A., Denlinger, R. P., 1978, Seismic Reflection and Gravity Investigations in a Geothermal Area, Stanford University Dept. of Geophysics, Final Technical Report USDI 14-08-001-15329.

Lee, W. H. K., Bennett, R. E., and Meagher, K. L., 1972, A method of estimating magnitude of local earthquakes from signal duration, U.S.G.S. Open File Report, 28 pp.

Lipman, S. C., Strobel, C. J., and Gulati, M. S., 1978, Reservoir performance of The Geysers field, *Geothermics*, v. 7, p. 209-219.

Lofgren, B. E., 1978, Monitoring crustal deformation in The Geysers geothermal area, California, U.S.G.S. Open File Report 78-597, 19 pp.

Lofgren, B. E. in press, Monitoring crustal deformation in the Geysers-Clear Lake region, in McLaughlin, R. J. and Donnelly-Nolan, J. M. eds., *Research in the Geysers-Clear Lake geothermal area*, U. S. Geological Survey Professional Paper 1141.

Majer, E., and McEvelly, T. V., 1979, Seismological investigations at The Geysers geothermal field, *Geophysics*, v. 44, no. 2, p. 246-269.

Marks, S. M., Ludwin, R. S., Lowie, K. B., Bufe, C. G., 1978, Seismic monitoring at The Geysers geothermal field, California, U.S.G.S. Open File Report 78-798, 26 pp.

McLaughlin, R. J., 1977, The Franciscan assemblage and Great Valley sequence in The Geysers--Clear Lake region in Field Trip Guide to the Geysers-Clear Lake area, Cordilleran Section of the Geological Society of America, p. 3-24.

Peppin, W. A., Bufe, C. G., 1980, Induced(?) versus natural earthquakes:

Search for a seismic discriminant, Seismological Society of America

Bulletin, v. 70, no. 1, p. 269-282.

Reed, M. J., and Campbell, G. E., 1976, Environmental impact of development at

The Geysers geothermal field, U.S.A., in Proceedings, Second United

Nations Symposium on the Development and Use of Geothermal Resources, p.

1399-1410.

## ACKNOWLEDGEMENTS

The authors are indebted to the reviewer, Dr. Douglas Stauber, for his many valuable comments. Dan O'Connell and Peter Shearer were of great assistance with last minute details, and David Oppenheimer made useful suggestions. Up-to-date data was provided by the California Network. Finally, we thank the Department of Energy which provided partial support for our work under memorandum of understanding BE-A108-76DP00474.